Section 1. Abstract.

A gamma-ray spectrometer employing a solid state gamma-ray detector of lithium drifted Germanium has been assembled and spectrometry results of good resolution have been obtained with the system for the gamma rays and positron annihilation quanta resulting from the radioactive decay of the sodium-22 nucleus. It has been found that the energy resolution obtainable with the system is similar to that in the systems of other workers and is somewhat better at the higher energies measured. Results have also been obtained for the intrinsic efficiency of the detector for gamma-ray detection as a function of source to detector distance and at different energies of gamma-radiation.

This thesis contains an account of this work, which should provide a useful introduction to the subject for anyone carrying on the author's work, as well as some detail on some of the finer points involved in the data analysis and theory of operation of the spectrometer.

Section 2. Acknowledgements.

I should like to express my appreciation to several members of the Physics Department of Ottawa University for assistance and support during the carrying out of this work. First I should like to thank Dr. Ian Fairweather for his always willing help and encouragement and for the frequent benefit of his knowledge of gamma - ray spectroscopy techniques; I must also acknowledge the fact that these measurements could not have been made without the generous provision of equipment, namely the electronics and the detector, from the research grants of Drs. Fairweather and Robson.

Although my relations with Drs. J.C.Woolley and R.C.Smith were unconnected with this research project in itself, I owe to each of them a debt of gratitude in having had the opportunity of demonstrating third year electronics in Dr. Wooley's laboratory class, during which my grasp of that subject was considerably strengthened, and in following some of the best physics courses I have had the privilege of taking, those given in the fourth year and to graduate students by Dr. Smith. Professor J.M.Robson read and gave some helpful comments on the main part of this thesis, Section 6, when it was in manuscript form.

I gratefully acknowledge the award to myself of an Ontario Postgraduate Fellowship, held during the academic year 1965-1966, by the Ontario Department of University Affairs; I am also thankful for financial support in the form of Graduate Assistantships from the University of Ottawa during the academic years 1964-5 and 1966-7.

Finally my appreciation is due wholeheartedly to the friends and acquaintances I made at Ottawa University on first arriving in Canada and subsequently, including those members of the workshop staff who have been so willing and able to assist in the making of apparatus and giving

of advice on technical problems, in particular Messrs. P. Azmier, R. Hart, and D. Kingswell. My thanks go to my fellow graduate students for their comradeship and moral support, amongst whom I must name Drs. J.Ancsin and J.Kos for their assistance and advice on setting up the low temperature thermometer in the cryostat, and Mr. Charles Spira for his patient instruction in some of the rudiments of practical electronics.

Section 3. Table of Contents.

Section 4. List of Illustrations.

Section 5. List of Data Tables and Graphical Results, and Appendices.

(a) Intrinsic Efficiency data preceded by explanatory note; graphs giving intrinsic efficiency as a function of source-detector distance for mercury-203 and Caesium-137 sources.

(b) Gamma-ray spectrometry results, including data derived from calibration of analyser. Appendix 1. on analysis of errors in the linear interpolation procedure used to find the unknown energies. Graphs 1-5 giving analyser (pulser) calibrations and detector response linearity relations.

(c) Energy resolution data and plot of relation giving Fano factor of germanium.

(d) Appendix 2. On heat transfer between concentric cylinders at reduced pressure.

(e) Representative examples of spectral peaks used in efficiency measurements.

Section 6. An Account of the Research and Results:

Chapter 1. Introduction.

Chapter 2. Apparatus.

Chapter 3. Results: an account of the experimental procedures and methods of calculation.

Chapter 4. Discussion of Results, with reference to similar work of others.

Chapter 1. Introduction.

In this chapter a brief discussion of the features of nuclear physics which explain the operation of solid state detectors will be given, highlighting the reasons for the performance obtainable from Ge(Li) devices in gamma spectrometry. An account of the main steps in detector development which have lead to these devices is also given, followed by a short description of the work undertaken by the author at Ottawa University to develop a semiconductor gamma-ray spectrometer.

The operation of lithium drifted germanium detectors with their inherent high resolution energy measurement capabilities relies, from the nuclear physicist's viewpoint, on two well known areas of text-book nuclear physics. These are the mechanisms by which gamma-rays interact with the matter of which the detector is composed, and the statistical theory underlying the attainment of energy measurements with small standard deviation. The problems in solid state physics associated with attaining the high resistivity intrinsic region in the detector, where the radiations are stopped, are left aside at present.

Gamma-rays interact with matter chiefly by three well known mechanisms, in each of which photons are removed from their original path by a single interaction; this fact implies, incidentally, that the intensity of gamma rays in anarrow beam will fall off exponentially with distance in traversing matter of uniform composition and density. The three mechanisms lead to separate absorption coefficients which can be added to give the total absorption coefficient which multiplies distance to give the exponent in the exponential intensity-distance relation.

Each of the three mechanisms involves production of secondary radiation, electrons which then lose their energy by multi-interaction processes in the material, and the relative efficiencies of the three processes depend both on the energy of the incident gamma-rays(E), and on the atomic number of the medium(Z). All three processes depend linearly on the number of absorber atoms per unit volume(N).

The largest effect in the low energy region, around 100 kev, is the photoelectric effect in which a gamma-ray transfers all of its energy to an electron which is initally bound in an atom. These photoelectrons are produced in matter by gamma-rays, X-rays, and even visible light, as in the photomultiplier tube cathode. The probability of photoelectric absorption, expressed by means of the linear absorption coefficient,(z(photo)), varies as

$$NZ^5/E^{3.5} \quad cm.^{-1}$$

A photoelectric interaction in the detector is registered by a pulse in the electronics which contributes to the full energy peak in the pulse spectrum stored by the analyser memory. (For a description of the common spectral features in multichannel analysis of gamma-ray spectra the reader is referred to the very useful section on principles of pulse-height analysis in the instruction manual for the 512 channel analyser published by Nuclear Data Inc.)

The second mechanism is the Compton effect, in which a photon strikes an electron and ejects it in one direction whilst being scattered with reduced quantum energy in another. The change in wave number of the photon, from k to k', is given by

$$1/k' - 1/k = (h/mc)(1-\cos C),$$

where C is the scattering angle of the Compton scattered photon. The corresponding change in energy of the photon occurring at the scattering event, from E to E', is given by

$$E' = E/(1 + (1 - \cos C).E/mc^2).$$

The Klein-Nishina formula gives the absorption coefficient, z(Compt.), for the Compton process at energies above 1 Mev. as approximately equal to

$$1.25 \times 10^{-25}.N.Z / E.(\ln 2E / mc^2 + 1/2) \text{ cm.}^{-1},$$

Thus z(Compt.) has very nearly an inverse dependence on E, and a direct dependence on electron density, each electron in the absorber contributing independently. As explained earlier, this absorption coefficient only applies strictly in the case of attenuation of a narrow beam, where single interactions remove quanta completely from the beam. For detector efficiency calculations allowance must be made for the fact that successive Compton scatterings of the same photon can give rise to complete absorption in the detector and a consequent charge pulse which appears to the electronics just like that from a photoelectric absorption of the gamma-ray. In such cases z(Compt.) is effectively decreased and z(photo) increased.

The third process, pair production, occurs when gamma-rays are annihilated in the vicinity of a nucleus, creating an electron and positron pair. Since the rest mass energy of the pair is $2mc^2$, the minimum value for E for which this occurs is 1.02 Mev. Pair production from gamma-rays above this energy results in electrons with total kinetic energy almost equal to the excess of E above the rest mass energies, since the nuclear recoil energy is very small. The pair-production absorption coefficient at energies near the threshold for the process varies as $N.Z^2 (E - 2mc^2)$.

Since the mean lifetime of the positron is very short in matter, ending in the inverse process to pair-production and consequent emission of two gamma-rays of energy equal to the electron rest-mass energy, (mc^2), all gamma-rays of energy greater than 1.02 Mev. are accompanied

by some of energy 0.51 Mev when they are absorbed.

From the above some important factors relating to gamma-spectrometry with semiconductors emerge. First, the ratio of the photoelectric coefficients for Germanium and for Silicon is about 40 for energies in the 100 Kev region due to the strong Z dependenee of z(Photo). Furthermore, the ratio of z(Photo) to z(Compt) varies as Z^4 for a given energy, and the ratio of pair-production coefficient to z(Compt.) varies as Z. These tendencies indicate the use of Germanium(Z= 32) in preference to Silicon(Z = 14) in order to achieve greatest absorption with least interference in spectra by Compton backgrounds.

The ion pairs, created by the slowing down of the high energy secondary electrons in the high resistivity depletion layer of the detector(diagram 1), are collected by the electric field existing in this region due to the application of a high voltage to the electrodes. The number of ion-pairs and thus the charge collected at the detector's electrodes, and eventually the pulse height in volts, after linear amplification in a charge sensitive preamplifier and pulse-shaping main amplifier, is directly proportional to the energy of the photon which gave rise to the ions, for a given detector material.

This proportionality between signal amplitude and deposited energy arises from the constancy of the average energy needed to create an ion pair, with respect to the energy deposited in the crystal by the radiation. This constancy means that, whatever the energy of the radiation, within reasonable limits, a constant fraction of it is used to create ion pairs in the lattice which can be collected at the electrodes as a charge signal; the remainder of the energy goes to excite

atoms without ionisation and is thus dissipated in thermal heating of the lattice.

However, since there is this variety of ways in which the radiation's energy can be expended in the lattice, the actual number of ion pairs formed from monoenergetic radiation stopping in the detector is subject to statistical variations which, in the hypothetical limiting case where ionisation becomes a rare event amongst the other energy dissipating mechanisms, would obey Poisson statistics. In the present situation we do not however approach this extreme and the variance in the number of ion pairs created during a detection event is smaller than its value in the hypothetical limiting case by a multiplying constant known as the Fano factor. The means of deducing F from energy resolution data is given in chapter 3, and the results obtained for the F value of Germanium are in section 8 of this thesis.

Since the average energy needed to produce an ion pair in Germanium is only 2.85 ev., compared with about 30 ev. for gases and 300 ev. per photoelectron in a scintillator-photomultiplier combination, the signal is about 10 times that in gases and 100 times that at the photocathode of a photomultiplier; the statistical fluctuations as a fraction of signal from the detector will therefore be less by a factor of three over an ion-chamber's signal and about twenty over a NaI(Tl)-photomultiplier signal. Thus, by using semiconductors, considerably greater energy resolution has been attained in nuclear particle spectrometry.

The development of the Ge(Li) detector has followed a logical series of events in the use of semiconductors first for detection of heavy charged particles, with p-n junction and surface barrier detectors, and thence, with the ability to produce detectors with

thicker sensitive regions by means of the lithium drifting process, for measurement of electron and gamma-ray energies, initially with Silicon as the basic material. However, the low photoelectric absorption coefficient for Silicon restricted the use of that material, for gamma-spectrometry, to the 100 Kev. region. The first instance of the use of the Lithium drift process in Germanium is recorded by Freck and Wakefield(1) who made a detector with an area of 1.5 $cm.^2$ and thickness 1.5mm., which gave an energy resolutiom of 3.2% at 662 Kev. This was followed by the work of Webb and Williams (2), and Ewan and Tavendale, much of whose work is discussed in their comprehensive article (3); they developed larger detectors and obtained much higher energy resolution in gamma-ray spectrometry.

The chief advantages of the Ge(Li) gamma spectrometer over the sophisticated curved crystal spectrometer of Dumond are its relative simplicity, higher intrinsic efficiency, and its ability to record an entire spectrum at once rather than as a single channel device. Comparing with the much used NaI(Tl) spectrometer, energy resolution for measurements above 500 Kev. is about twenty times better. i.e. energies can be found with a precision of 0.3Kev, as will be shown in the present work, instead of , typically, 6Kev. with NaI(Tl). In addition, the collection time, around 30 nsecs., for charges released by ionisation in the detector are an order of magnitude faster than pulse rise times from a scintillator. This enables smaller coincidence resolving times to be achieved in the detection of coincident events. However, the full energy peak efficiency is generally much lower for Ge(Li), due to the limited depth of depletion layer attainable at present. Newer, coaxially drifted detectors, described by Malm et alia(4), are being manu-

factured at present with similar volumes and efficiencies to small sodium iodide crystals.

In the present work, energy resolution measurements have been made on gamma-rays with known energies in the range 122 Kev.(Co 57) to 2614Kev.(Tl 208), with results close to the values obtained by Ewan and Tavendale(3) in measurements at 122, 1333, and 2614 Kev. By means of finding the channel numbers of the peaks recorded by the analyser as a function of the energies of the corresponding gamma-rays, and also the channel numbers of peaks produced from electronically produced pulses of known heights, gamma energies are correlated with pulse heights in volts. The resulting detector response relation is very nearly linear and is used to find unknown gamma energies by interpolation between primary standard energies. In this way the Na-22 gamma-ray has been remeasured with similar precision to, and in agreement with a measurement using identical techniques by Robinson, Stelson, and McGowan (5), and the energy of annihilation quanta has been found and agrees with the rest mass energy of the electron as established by Dumond et alia(6), to within the standard deviation of about 0.3Kev.

An important parameter for any nuclear radiation detector to be used for absolute counting measurements is its intrinsic efficiency or the fraction of particles or rays striking it which are eventually recorded by the system. The photopeak intrinsic efficiency has been calculated for the Physics Department's 3.7 cc. cylindrical detector as a function of source-detector distance and for gamma-rays of two energies in the 100Kev. to 1Mev. region. Results agree with those of Ewan andTavendale (3), made for a fixed distance between source and detector, to within 7%.

From the quantity of full energy peak half width data that has been obtained for various sources, the Fano factor of the detector material has been deduced from the linear relation existing between the square of the statistical uncertainty in an energy measurement and the energy itself. This relation arises from the statistical nature of the number of ion pairs, mentioned above, and is discussed at greater length in Chapter 3(c).

Chapter 2. Apparatus.

(a). The Detector.

Semiconductor radiation detectors are solid state versions of the classical ionisation chamber which works on exactly the same principle: the production of ionisation and the collection by an applied electric field of electron-hole pairs created by the energy deposited by the detected radiation in the lattice of the semiconductor . This electron-hole pair collection corresponds exactly to the similar process of collection of ion pairs in the gas of an ionisation chamber. However, as mentioned earlier, greater energy resolution, i.e. relative uniformity of pulse amplitudes arising from detection of monoenergetic gamma-rays, is achieved with semiconductors than with gases since, on average , about ten times as many charge pairs are created for a given quantity of energy deposited .

Diffusion of a donor element, say phosphorus, from the vapour phase into a piece of high resistivity p- type bulk Silicon or Germanium is used to produce the p - n junction detector which will detect radiations which step in its depletion region. However, the thickness of this region, when the device is manufactured from readily available materials, is limited to about half a millimeter, and thus suffices for detection of medium energy electrons or heavier particles only, and cannot be used for gamma- detection . In a case where the n-region doping is very heavy , as in all radiation detector situations, almost the entire junction voltage drop appears in the p - region and the width of the depletion layer is given by

$$W = (K.V / 2\pi e N_a)^{1/2}, \qquad \text{Ref. A, p. 128.}$$

where K is the material's dielectric constant, V is the voltage applied across the junction , and N_a is the net density of charge carriers which is inversely proportional to the resistivity. (It can be shown

that the depletion region extends on either side of the junction of p and n materials in the junction counter and that the extensions on either side of the junction are directly proportional to the respective resistivities in the two regions away from the junction.(Ref. A). Thus, in junction and lithium drifted detectors where the resistivity of the p-material is much higher than the resistivity in the heavily doped n - region, the depletion layer falls mainly on the p - material side of the junction when the reverse electrical bias is present.)

The width of the active region is thus limited by the voltage which can be applied to the junction without some form of electrical breakdown, and by the number of acceptor sites.

In Silicon and Germanium prepared by the normal zone refining processes sufficiently high resistivities cannot be attained to give deep depletion layers, with the depths of 1/2 cm. or more required for gamma ray detection. However , high resistivity material can be made by effectively cancelling out some of the negatively charged acceptor sites in the p-type bulk material with positively charged lithium ions located interstitially in the lattice.

This is achieved by the so called lithium- drift process in which Lithium is usually evaporated onto the surface of the p-type semiconductor material and is then allowed to diffuse into the surface at a temperature of about 400°C, forming the thin n^+ layer shown in Illustration 1. Applying a reverse bias then causes positive Lithium ions to move from the thin surface diffused region into the bulk of the detector, compensating acceptor atoms en route. The low ionisation energy of Lithium atoms and the high mobilty of Lithium ions in semiconductor lattices allows this process to take place at a reasonable rate which is also simply predictable. The theory of this process is well documented and a clear account is given in the very

informative paper , by F.Goulding , Reference 11. Depletion layers in planar detectors with depths up to 1 cm. are thus quite commonly used now , and with such active volumes a reasonable intrinsic efficiency, of the order of a few percent for full energy gamma detection , can be achieved. An added advantage with thicker depletion regions is that the capacitance is not so great as to seriously degrade the energy resolution given by the electronics . The junction capacitance for a Germanium detector is given by (1.40 A/W) pfd. and thus is about 11 pfd. for the detector used here. A further 3 pfd. has to be allowed for capacitance arising from the metal encapsulation and 2.4 pfd. for the high voltage lead built into the cryostat.

At room temperature Lithium atoms tend to precipitate at vacancies in the lattice and thus become electrically inactive . This effect appears to be greatly reduced at liquid nitrogen temperature , presumably due to the fact that Lithium ion mobility in the lattices decreases as the temperature is lowered . This is one of the reasons for use of a vacuum cryostat in which the detector is mounted and operated at reduced temperature , as described in the next section of this chapter.

A further experimentally important quantity associated with a detector in operation is the collection time for charge carriers making the complete transit across the depletion layer, which is given by

$$T = (W^2 / u.V),$$

where u is the ion mobility in the electric field due to a voltage , V, across the layer of thickness W. Using mobility data in Ge at 77°K the collection time and thus the pulse rise times for charge flowing from the detector is about 14 nsecs. for an applied potential of 900 volts , as used in all the work described here.

(b). The Cryostat.

For the successful operation of Lithium drifted Germanium detectors they must be cooled well below room temperature for two reasons. First, at room temperature Lithium atoms are sufficiently mobile in the Germanium lattice to precipitate at vacancies and thus become electrically inactive and fail to produce the necessary compensation at the acceptor sites of the p-type base material to form the intrinsic region. Secondly , because of the smallness of the energy gap between valence and conduction bands (0.66 eV. at 300°K.), the number of thermally generated electron hole pairs, and consequently the reverse current in the diode when an electric field exists in the depletion region, is considerable. This reverse current produces a contribution to the overall spreading and concealing of the wanted signals which results in the limit on energy resolution obtained in the system. This reverse current must , therefore be kept to a minimum by cooling the detector , preferably to liquid nitrogen temperature, when the reverse current should be in the region of 10^{-9} to 10^{-8} amps under operating conditions,(v. Refs. 1 &8). Measurements of reverse current were not made by the author , but since the detector operated with the energy resolution expected under optimum conditions it was assumed that reverse current was sufficiently low. The silicon device will operate satisfactorily at room temperature , but for reasons mentioned earlier cannot take the place of Germanium for much nuclear physics work.

For these reasons the Germanium detector has to be mounted , when operating , in a cryostat capable of reducing and maintaining its temperature for extended periods near that of liquid nitrogen. A cryostat of the type shown in Illustration 3. was used, built to the design given in reference (9), and the detector was mounted on the pedestal

of aluminum which gives minimal back-scattering because of its low mass number. The pedestal was attached and cooled to the temperature of one end of a Copper"cold finger", the other end of which is immersed in liquid nitrogen kept in a 25 - liter Dewar, a sufficient capacity for the system to be left untended for periods up to 10 days or so. The temperature reached under operating conditions at the detector was measured by means of a Copper resistance thermometer, wound around the shaft of the pedestal. The calibration , by Dauphinee and Preston - Thomas , of this type of thermometer wound on a Copper calorimeter, was used as the basis of present temperature measurements (REfce. 10). However , in this case the Copper wire was wound, with the very minimum of tension in the wire to preserve its electrical characteristics, on to the aluminum pedestal of the cryostat; due to the difference in constructional material between wire and pedestal a small degree of differential thermal expansion was introduced. However, a check on the accuracy of the thermometer was made by immersing the complete pedestal and coil assembly in liquid nitrogen, and recording the temperature given by the ratio of coil resistance at that temperature to the resistance at 0°C. Thus the temperature of the immersed coil was found to be about 100°K, and this was accepted as sufficient evidence of the thermometer's satisfactory performance in the relevant temperature region. The difference of the reading from liquid nitrogen temperature may well have been due to the fact that the coil was completely wrapped in masking tape to keep the coil secure whilst suspended in a vacuum flask. When the pedestal was incorporated in the coolad cruostat, at working conditions of between 10^{-3} and 10^{-4} torr air pressure inside, the coil temperature was found to be almost exactly the same as in the check measurement, i. e. at about 105°K. This temperature is in good agreement with that found by

Chasman and Ristinen for their evacuated cryostat, (REF. 9), about an hour after immersing the lower end in liquid nitrogen. In order to protect the Germanium detector from possible thermal shock during these preliminaries the detector was simulated inside the cryostat by means of a cylinder of mild steel of identical dimensions to those of the actual detector. In order to maintain these temperatures inside the cryostat for appreciable times,and with reasonable liquid nitrogen economy, the assembly had to be evacuated by means of a rotary pump to about 10^{-3} torr and then finally pumped down with molecular sieve built into the cryostat , to pressures in the region of 10^{-4} torr where heat transfer across spaces of the dimensions of the inside of this cryostat is very low and is by free molecular conduction , rather than the thermal conductivity mechanism existing at higher pressures , together with radiative transfer. Radiation is actually the predominant mode of heat transfer in air at these pressures. A calculation given in Appendix 2. shows that at 10^{-3} torr free molecular conduction and radiation account for about equal amounts of heat transfer , whereas at 10^{-4}torr radiation is predominant by a factor of twenty. At these pressures the thermal conductivity decreases linearly with the pressure. (Reference C).

It was shown in the author's work that the temperature at the detector site rose only as far as 125°K. even when the vacuum was as poor as 10^{-2} torr and 145°K. at 0.5 torr.

Once the vacuum had been produced in the cryostat it was monitored by a vacuum gauge operating with either a thermocouple type gauge head or a Balzer ionisation gauge head . Beside achieving low liquid nitrogen consumption a good vacuum is also a good assurance against the deposition of any electrically conducting material on the outer

surface of the detector capsule, thereby possibly raising the leakage current to a level at which it introduces excessive noise into the signal pulses.

One extra requirement of this cryostat is a low capacitance lead for H.T. and signal between an insulated terminal on the cryostat case to the live terminal on the detector. (Illustration 3.) As a preliminary to constructing such a lead inside the cryostat, the theoretical capacitance was calculated for possible configurations involving variations in lead diameter , insulation material, and lead to case spacing . The lead finally used was of very fine Tungsten wire, 3 thousandths of an inch in diameter, glued inside a section of polythene tubing in such a way that it was under slight tension, and thus possible capacitance change or vibration arising from disturbance of the cryostat was avoided. The polythene tube and wire was then attached to the inside of the cryostat case and the ends of the wire , which had been previously Copper plated and tinned, were soldered to the respective terminals. As a final check the capacitance was measured using a Boonton Q - meter and found to be 2.4 pfd., rather higher than the calculated figure of about 1 picofarad but nonetheless compatible with the mutually parallel capacitance of the detector, i. e. 14 pfd.

Finally, mention should be made of the fact that mounting the detector in the cryostat in such a way that the detector was at room temperature for as short a while as possible was a process requiring a certain amount of ingenuity. It involved mechanical mounting of the detector, with a mounting ring and screws,to the pedestal, soldering of the H.T. lead in place, then final assembly of the cryostat with detector in situ, checking for electrical insulation between H.T. lead and case after assembly, and finally the fairly lengthy procedure of evacuation to

around 10^{-4} torr. The latter process involved first the evacuation from atmospheric pressure to a pressure in the region of 10^{-3} torr with a Balzer's rotary vacuum pump, simultaneously with heating of the stainless steel tubes of the cryostat and the contained zeolite adsorbing agent by means of a hot air blower; after it was estimated that degassing was complete, the cryostat was allowed to cool to room temperature and then to liquid nitrogen temperature by immersion of the cold finger in the vacuum flask of liquid nitrogen. During the heating of the stainless steel tubing with hot air, the Copper cold finger extension, which screwed into the bottom end of the cold finger indicated in diagram 3, was immersed in an ice-water bath to keep the detector at its upper end as cool as practically possible during this time. The temperature of the detector was also monitored by means of the Copper resistance thermometer during this period to ensure that it did not rise significantly due to the heating. Upon final immersion of the cold finger in liquid nitrogen, the time taken for the upper end to reach its equilibrium temperature of around 100°K. is about one hour (Ref. 9), an adequate period to ensure that the detector does not suffer from thermal shock during the cooling from room temperature to 100°K.

(c). Electronic Equipment .

In order to fully reap the advantages inherent in semiconductor detectors the ancillary electronic equipment has to be well suited to their characteristics. This applies particularly to the achievement of optimum resolution and speed of response in the detector's output signals . A block diagram (Illustration 4.) of the electronic equipment used is given in section 7.

Since the events detected are measured as pulses of electrical charge collected at the electrodes of the detector , which behave also as the plates of a capacitor, the heights in volts of pulses appearing at the detector electrodes vary with the capacitance of the detector as well as with the quantity of charge in the pulse. Since the depth of the depletion layer is a function of the applied voltage , the detector capacitance varies with any fluctuations in the high voltage supply . A voltage sensitive preamplifier would thus be of little use to amplify the signals coming directly from the detector , and a device which gives an output pulse whose amplitude is proportional as nearly as possible to the charge in the input pulse is needed. This is achieved by means of a feedback capacitor , C_f, in parallel with the first amplification stages of the preamplifier , which causes the input capacitance to the amplifier to be $(A + 1). C_f$. This can be shown by an approximate analysis of the feedback loop, assuming infinite input and zero output impedances, and open loop gain A. The design of the preamplifier is therefore such that $(A+ 1).C_f$ is much greater than C , the combined detector and stray capacitance from the connecting lead,(q. v.), and input circuit capacitance of the preamplifier . When this inequality holds true, any changes in the detector capacitance due to variation in thickness of depletion layer are effectively swamped

by the large capacitance appearing at the input of the preamplifier.

The output voltage signal from the charge sensitive stages is then given by

$$V_o = Q / C_f,$$

and is typically about 50 Millivolts per Mev. of gamma radiation energy deposited in the detector when the feedback capacitor in the preamplifier is 1 picofarad. The open loop gain was 5000 for the preamplifier used here, making (A+1). C_f considerably larger than the total input capacitance to the preamplifier of about 20 pfd., including detector capacitance.

The remainder of the electronic units further process the pulses from the preamplifier which have height in volts given by ($a.Q / C_f$) when charge pulses, Q, flow from the detector into the preamplifier, with feedback capacitor C_f determining the charge sensitive gain, and a further amplification by a factor "a" applies for the stages following the charge sensitive part.

A further overall voltage gain factor, G, is applied by the main amplifier , together with some pulse shaping, discussed below, giving an output voltage for pulses at B (Illust. 4.) of (GaQ / C_f). The biassed amplifier is then capable of removing the lower portion of the pulses, below a voltage level which can be adjusted by an external control , and then amplifying , by gain factors up to 20, the remaining top parts of the pulses. This process enables series of pulses which differ only slightly in height at the input of the biassed amplifier to be clearly distinguished at the output. With the instrument used here the range of levels over which biassing could take place was 0 - 10 volts . Labelling this arbitrarily set level as L volts , and the gain subsequent to biassing as g, the pulses at C and T have height

$$(GaQ / C_f - L) . g$$

Pulses at this point, of differing heights corresponding to the various values of Q, for different quantities of deposited radiation, are recorded in the 400 channels of a multichannel analyser, the number of the channel in which a pulse is counted being linearly related to the mean of a small range of heights of input pulses. The number of pulses recorded in any one channel is proportional to the spectral density of pulses in the corresponding region of detector pulse heights. Neglecting the finite width of the channels theanalyser is designed so that there is as near a linear relation as possible between the pulse height and its corresponding channel number.

Since the pulses are required to pass through the electronic system with as little change in shape as possible , except for deliberate pulse - shaping in the main amplifier, the inputs of the various units must be impedance matched to the interconnecting cables which were of 93 ohms characteristic impedance in all of this work. The input impedance of 125 ohms of the main and biassed amplifiers thus necessitated parallel resistors at their inputs , attached with B. N.C. connectors and T-junctions, to reduce the apparent z(input) to 93 ohms. This avoids reflections of parts of the pulses at terminations of the cables and the resultant "ringing" of the pulses. Slight variations in heights of pulses originating from monoenergetic gamma-rays arise from the various sources of noise discussed elsewhere in this thesis, but these variations require other methods of reduction which are often difficult indeed to achieve : the literature of the last three or four years shows the great volume of work that has gone into development of these high resolution systems by leading workers. These latter variations are manifested in the finite widths, usually

of several channels, of the spectral peaks recorded and displayed by the analyser, when the electronic pulser feeds the system.

Differentiating and integrating pulse shaping circuits are used in the main amplifier in order to prevent pile up of pulses and to improve the signal to noise ratio of the pulses by attenuating a part of the electronic frequency spectrum over which only a little of the signal is spread but which contains a significant proportion of the noise. The differentiating circuit , in which the input signal is applied to a series combination of resistance and capacitance , and the output taken from across the resistor only, acts as a high pass filter which does not reduce noise , but shortens the duration of the pulse, bringing it back to baseline level rapidly after reaching its maximum amplitude. This reduces possible pulse pile-up when counting rates are high. The integrating circuit , however, in which the output is taken from across the capacitor in the R-C series combination, does reduce the noise fraction in the signal since it acts as a low pass filter and the fraction of the noise occupying the high frequency region is attenuated. In the author's work the amplifier was used with values of shaping time constants which were experimentally found to give the best resolution in spectrawhich were recorded by the system for pulses from the electronic pulser adjusted so that its output simulated Co - 60 gamma ray pulses from the detector.

There are two chief sources of the total noise apart from that associated with the statistical spread of the detector signal, which is discussed in chapter 3. They are (1), the shot noise in the reverse current flowing in the detector , which is effectively in parallel with similar fluctuations in the input current to the first amplifying device, and (2), the noise developed in the first amplifying device which can be treated as Johnson noise in the equivalent input noise

resistance in the amplifying device. Beside these sources there is the surface leakage current on the detector which contains noise that is not of a well known type such as shot or Johnson noise. It is worth noting here that the electrical noise sources , which in the better preamplifiers introduce a line width (F.W.H.M.) of about 2 Kev. energy equivalent, are equal in magnitude to the statistical effect in Germanium for gamma- rays with energy in the 1 Mev. region , and that below 100 Kev. these sources are easily predominant.

Chapter 3. Results.

(a) Intrinsic Detection Efficiency.

Spectra were recorded for gamma ray sources of known activities. (They were calibrated gamma sources supplied by the Division of Research and Laboratory of the International Atomic Agency in Vienna.) For each source the total counts under the full energy peak were found from the printed data output from the multichannel analyser for various distances between the source and detector, in each case with the source on the axis of cylindrical symmetry of the detector. The sources were selected so that a single gamma-ray was involved in each measurement, thus eliminating possible complications in allowance for background resulting from the Compton distribution region of the spectrum of a gamma ray of higher energy which might be present otherwise. The photopeak from each gamma ray was made to occupy as many channels of the Victoreen 400 channel analyser as possible by using a biassed amplifier after the main amplifier. The use of this device is mentioned further in chapter 2 of the thesis. Results were repeated at two distances with one of the sources, using first a retort stand clamp to support the source close to the stand, and then supporting the source at the end of a cardboard tube which separated it from any material of high atomic number. This procedure was carried out to ensure that the photopeaks recorded did not contain counts registered for gamma rays which had been scattered by material surrounding the source.

The total counts recorded in the measured live time of the analyser was corrected for background by subtracting the area under a straight line interpolated between the asymptotic parts of the spectrum outline curve at the high and low energy extremes of the

photopeak. Examples of the spectra are given which show this. The resulting total count was checked against the area of a true Gaussian peak with the same peak half width and height as the experimental peaks. Agreement within the statistical error in the total counts indicated that the shapes of the peaks recorded, and the background allowances, were satisfactory. The expression for the area under a Gaussian peak is $1.0665 p_0 f$ where p_0 is the count in the peak channel, and f is the peak half width in channels. This corresponds to a probability distribution for the numbers of the counts occupying the channels given by

$$p(E) = \left\{ N/\sigma(2\pi)^{1/2} \right\} \exp\left\{ -(E - E_0)^2/2\sigma^2 \right\}$$

where p(E) is the count in channel number E, N is the total counts under thepeak, E_0 the channel number for maximum counts and σ is the standard deviation in E. It can be shown that

$$p(E_0) = p_0 = N/\sigma(2\pi)^{1/2},$$

$$\text{i.e.} \quad N = p_0 f (2\pi)^{1/2}/2(2\ln 2)^{1/2}$$

The radioactive sources are effectively point sources at the distances which have been used, since the active material is placed between two thin polyethylene discs in the form of a drop of liquid initially. Thus the inverse square law can be applied for the reduction of radiation intensity with distance. The intrinsic efficiency, defined as the number of pulses registered in the photopeak as a fraction of the number of rays simultaneously striking the face of the detector facing the source, is therefore related to the overall efficiency, defined as the number of counts in the photopeak as a fraction of the total number of photons leaving the source in the same time, by the simple geometric relation:

$$(\text{Eff})_{\text{int}} \cdot A = 4\pi R^2 \cdot (\text{Eff})_{\text{over.}}$$

where R is the total distance, made up of the measured distance between source and the outer surface of the cryostat aluminum cap, and the

"window" on the detector itself, shown in diagram (2), and A is the area of the detector face.

The errors resulting in intrinsic efficiencies are the statistically combined result of errors in the known source strength, the gamma ray per disintegration factor for each source, the statistical uncertainty in the total counts from the spectra, and the error in measuring the distance R. Results in tabular form and graphs relating efficiency to distance are given in section 8, together with an explanatory note on the formula used for computing the efficiency.

(b). Gamma-Ray Spectrometry.

The equipment was set so that the spectrum of a group of gamma rays from various sources could be recorded and stored in the analyser's memory. The sources were selected so that the energy of the gamma ray to be measured fell somewhere within the range covered by the group. Spectra were recorded and the channel numbers corresponding to the various gammas present were read from the visual display. Spectra were also recorded for pulses from a pulse generator covering the same range of pulse heights as the detector signals from gamma ray detection. Peak channel numbers were taken for the peaks recorded by the analyser for the various pulses whose heights in volts were accurately measured by a differential voltmeter. In this way gamma energies and pulse heights in volts were related graphically to channel number and thus both known and unknown energies were related uniquely to voltages known with an accuracy of one part in 5000. The plots of E versus pulse height in volts are extremely linear, indicating the linearity of the detector's response, i.e. the number of charge pairs collected at the electrodes with respect to the energy of the radiation. This linearity allows simple interpolation (see Appendix 1.) between the known energies of two of the calibration lines to obtain an unknown energy. The channel number versus gamma energy relation , which is more simply obtained, is not expected to have this feature since linearity of amplification and analogue to digital conversion processes is also involved.

Graphs are given for energy regions as follows: between 835 & 1332 Kev., using Co-60 and Na-22, Mn 54 and Zn-65, and between 1173 and 1332 Kev. using Co-60 and Na-22 only, to find the higher energy gamma-ray from Na-22; and from 238 to 612 Kev. using Thorium(B+C+C"), Ir-192 and Na-22 to find the energy of the positron annihilation quanta.

Energies assigned by this method incorporate the uncertainties in the known energies of the calibration lines and the reading errors of the peaks in the spectra, which in this case amounted to a quarter channel width in all cases. An analysis of the statistical combination of these errors to give the error in the final result is given in Appendix 1. to this thesis. The quality of the results in comparison with the work of others is discussed in chapter 4. Numerical results found were 1274.1 ± 0.2 Kev. for the 1173 to 1332 Kev. data, 1274.2 ± 0.5 Kev. for the 835 to 1332 Kev. data, and 511.0 ± 0.3 Kev. for the 236 to 612 Kev. group. The maximum non-linearity in the detector response relations recorded is 0.5% in the low energy range and 0.1% in the higher range.

(c). The Fano factor for Germanium.

The resolution which can be obtained with the gamma-ray spectrometer is limited by noise arising from two sources, namely the purely statistical effect of the fluctuations in numbers of ion pairs produced in a detector by monoenergetic gamma rays, and secondly all sources related to signal fluctuations arising in the electronics of the system, such as the detector leakage current noise. It is the first effect , which is a fundamental limitation, which we are here concerned with. Since all sources of noise are random, and are statistically independent of one another, the total effect can be computed by adding the magnitudes of the various sources in quadrature. Thus, in order to find the experimental magnitude of the statistical variation in number of ion pairs the effects of all other sources must be deducted from the total. Denoting the various noise quantities, (full width at half maximum in kev. ,or equivalent numbers of ion pairs) as $N_{tot.}$, $N_{det.}$, $N_{amp.}$ for the total noise, detector noise, and amplifier noise respectively, we can write

$$N_{tot.}^2 = N_{det.}^2 + N_{amp.}^2$$

Now $N_{amp.}$ can be found by using electronically produced pulses with a very high degree of uniformity in height in place of the normal pulses from the detector, and observing the recorded spread in heights of these pulses after passage through the electronic system. To be quite rigorous here, the biassed detector should be attached to the preamplifier when this measurement is made in order that reverse current and surface leakage effects should be present. Thence measurement of $N_{tot.}$ for pulses produced from ionisation in the detector, with exactly the same amplifier pulse shaping time constants, gives $N_{det.}$ by subtraction in quadrature. $N_{det.}$ arises from the statistical variation in number of ion pairs produced in the detector when monoenergetic radiation is stopped in the depletion region. It is due to the fact that the prod-

uction of ion pairs along the paths of primary and secondary radiations in the crystal is a random process, analytically similar to the radioactive decay process in that the number of ion pairs produced along a given length of primary radiation path is subject to Poisson statistics just as is the number of disintegrations occurring in a large number of radioactive nuclei in a given time. However ,whereas the latter process is strictly random, the former is not since if all the energy were used in producing ion pairs in the crystal and there was thus no energy lost in excitation processes which do not contribute to the electronically observable signal, then there would be always an exactly similar number of ion pairs produced when a gamma- ray of a given energy was stopped. The degree of randomicity in the process is in fact linked to the degree to which ionisation events are rare. Thus we can say that in this physical situation ionisations are not completely random processes but are to some extent statistically dependent on each other and the variance in the numbers of such events is consequently somewhat less than the variance if the process were purely random. The factor by which it is less is the so called Fano factor.

Thus, if E is the gamma energy and w is the average energy needed to produce an ion pair in the lattice, which will be treated as constant with respect to E, the total number of ion pairs produced will be E/w and the variance will be (FE/w), where F is the Fano factor, since E/w would be the variance if the number were distributed according to Poisson statistics. The standard deviation in number of ion pairs will therefore be $(FE/w)^{1/2}$ and N_{det}(f.w.h.m.) is $2.35(FEw)^{1/2}$ where E and w are measured in Kev. Thus if $N_{det.}^{2}$ is plotted against E for measurements made with various gamma energies a straight line with slope 2.35^{2}x2.85F should result,

2.85 being the average energy per ion pair in Germanium (Ref. 3, p. 2287).

The energy band gap, between valence and conduction electron bands, in Germanium at 100°K, is 0.75 ev. and thus the degree to which energy is lost by lattice heating effects, outside of true ionisation processes, can be found by comparison with "w". Reference A cites (p. 22.) that Fano has shown that Fis in general less than $(1-p_i)$ where p_i is the probability of an ionising collision. From the above data for Germanium p_i is seen to be less than about one in four, this figure corresponding to a sequence of events in which one collision resulting in ionisation is followed by an average of about three excitation collisions each absorbing energy close to that needed for ionisation. Thus, according to Fano's theory a value for F in Germanium less than 0.75 is satisfactory. The results obtained here(Section 8) yield a value of 0.57 ± 0.10 for the Fano factor of Germanium.

Chapter 4. Discussion of Results.

The results for the intrinsic efficiency and Fano factor of the detector and the spectrometry results together with the energy resolution of the data obtained at various energies are given below, together with results obtained by other authors.

Gamma Ray Source	Energy (Kev.)	Data of Chaplin.	Data of Ewan and Tavendale.	
		Intrinsic Efficiency of the 3.71 cc. Detector.	Efficiency corrected to 4cc. (Ref. 4)	Given in Reference 3. for a 4cc. detector.
Hg^{203}	279.1	8.32%	9.0%	9.7%
Cs^{137}	661.6	1.88%	2.03%	1.9%
All efficiency measurements have been taken at a source-detector distance of 12.5 cms.				

The volume correction has been made by assuming a direct proportionality between detector volume and full energy peak efficiency. The evidence for this relation is given in Reference 4. The agreement between the above results is within approximately twice the standard deviation in the author's results. The Fano factor for Germanium has been found to be 0.57 ± 0.10 which is rather higher than the results quoted in references 3 & 11, but is below the theoretical upper limit of 0.75.

Spectrometry results are summarised in the following table together with the values obtained by others.

Source of earlier Result.	Earlier Result. (Kev.)	Present Result. J.A.Chaplin.
Reference 5: by Robinson, Stelson and McGowan.	1274.6± 0.3 1274.6 ± 0.3	1274.1 ± 0.2 (i). 1274.2 ± 0.5 (ii).
Reference 6: Cohen, Dumond et alia.	511.003 ± 0.005	511.0 ± 0.3

The results from reference 5 were obtained with a very similar apparatus to the present one, i.e. a Ge(Li) detector based spectrometer. The author's two results given for the higher energy have been determined from separate calibrations over the same energy range, and interpolating between the same primary standard gamma-rays. However, the first result was obtained from spreading a 159 Kev. range of gamma energy across the 400 channels of the analyser, whereas 498 Kev. were occupied in the same region in the less precise result. Hence the greater accuracy in the first case, since the definition of any spectral peak is at best (1/4) channel when measured by eye on the oscilloscope display of the analyser.

Energy resolution was found to be as follows for three well spaced lines:

Line Energy (Kev.)	122	1333	2614
Gamma-Ray Source.	Co-57	Co-60	Tl-208
Present Resolution. (f.w. h.m.)(Kev.)	2.43	3.70	5.04
Resolution obtained in Reference 3.	2.05	4.0	5.5

Thus the present system has given somewhat better resolution at the higher energies than the system used for the results given in reference 3.

Section 7. Illustrations.

1. Schematic Diagram of the Planar Lithium Drifted Detector.

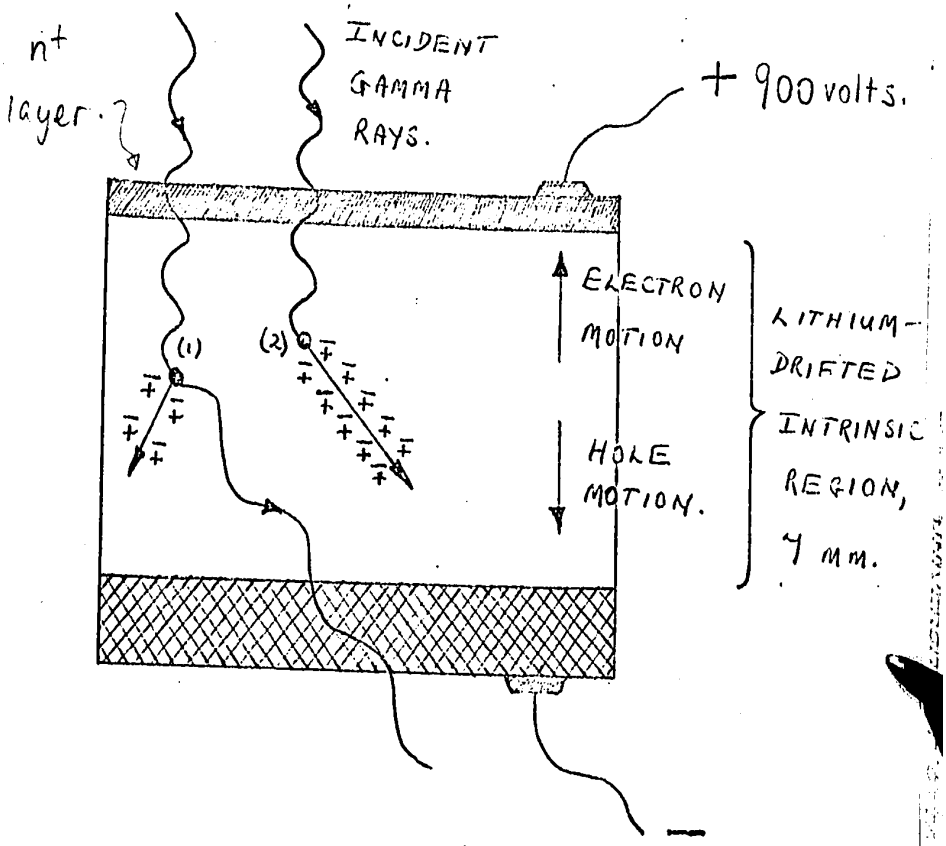

NOTE.

(1) is a Compton Scattering Event.

(2) is a Photoelectric Event.

Typical Base Material is p-type Germanium with resistivity approximately 10 ohm.cm. at room temperature.

2. Source Detector Geometry used in Efficiency Measurements.

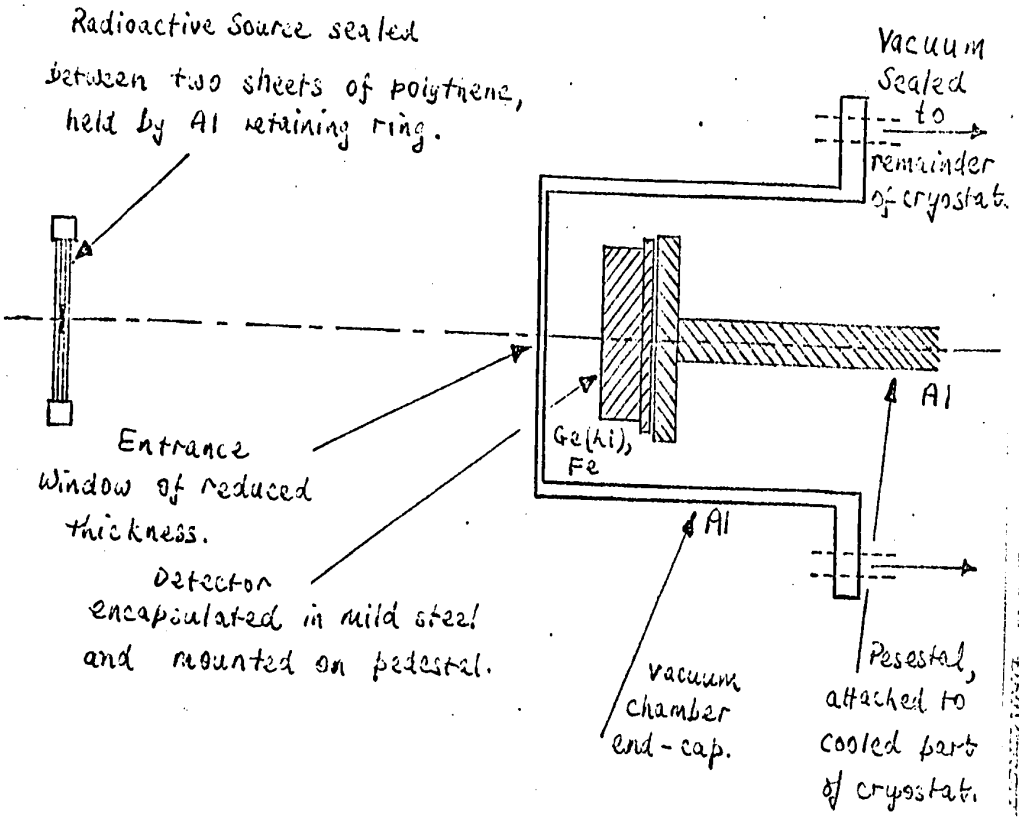

Constructional Detail of Detector showing Radiation Window onto Active Region.

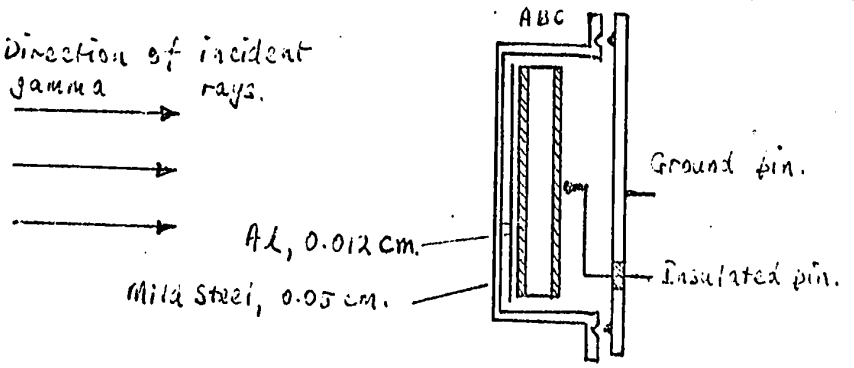

KEY: A is the lithium diffused side of the germanium detector (0.5 mm.)
B is the active volume of the germanium detector. (7 mm.)
C is the undepleted portion of the p-type germanium.

3. Cross-Sectional Diagram of Vacuum Cryostat.

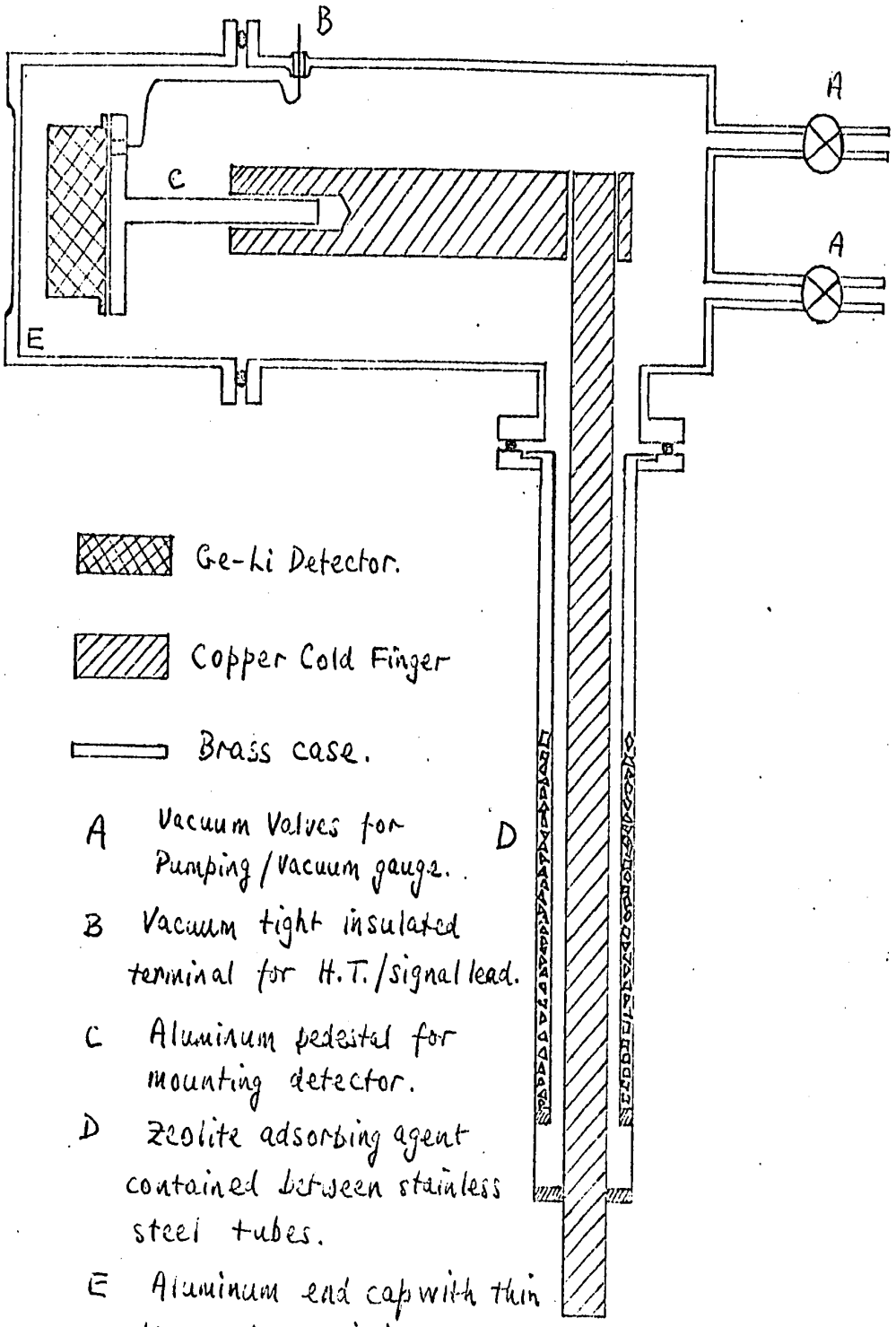

Ge-Li Detector.

Copper Cold Finger

Brass case.

A Vacuum Valves for Pumping / Vacuum gauge.

B Vacuum tight insulated terminal for H.T./signal lead.

C Aluminum pedestal for mounting detector.

D Zeolite adsorbing agent contained between stainless steel tubes.

E Aluminum end cap with thin layer for radiation window.

4. Block Diagram of the Electronic Equipment, with pulse heights indicated at various points.

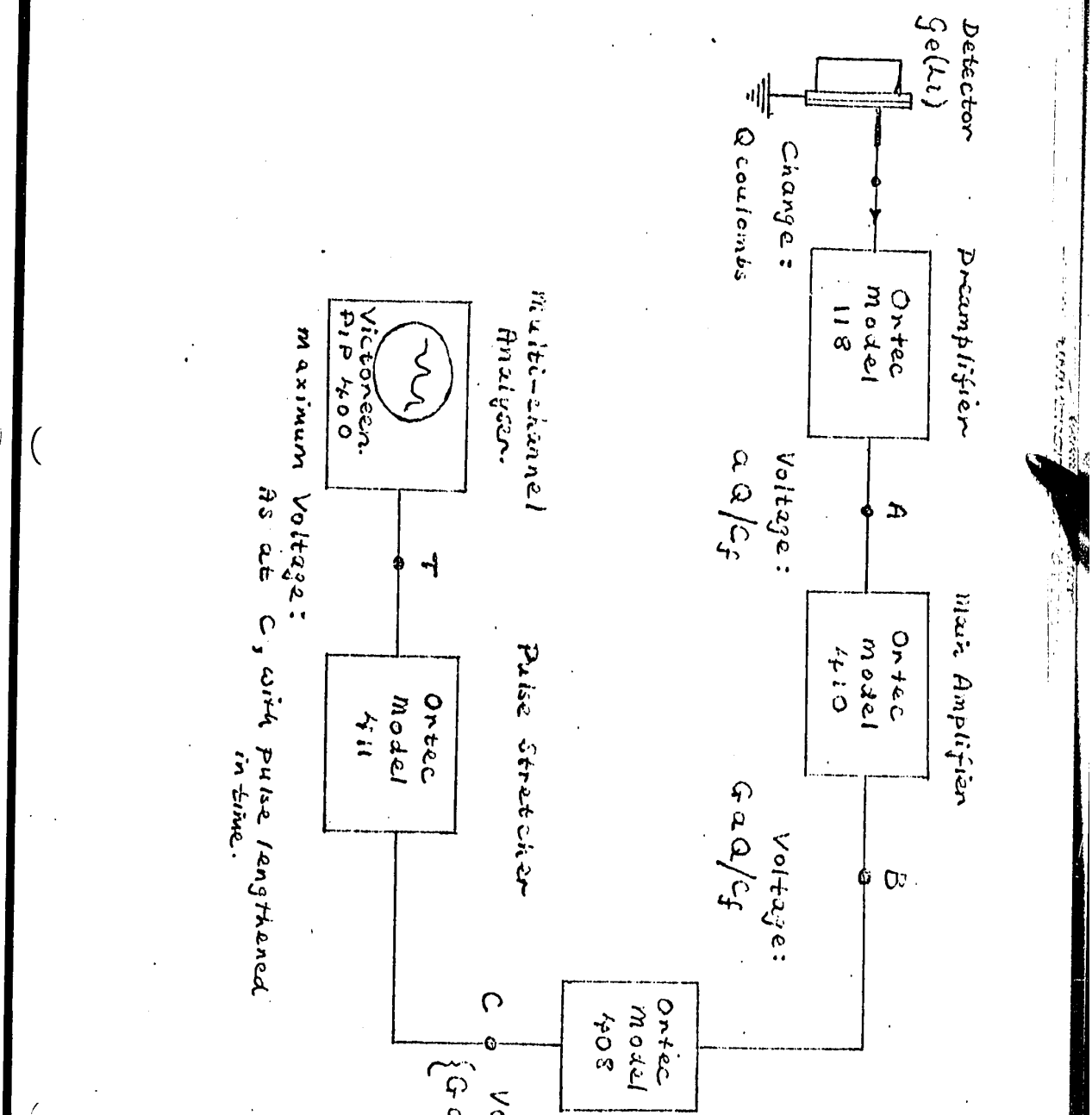

Section 8. Data Tables, Graphs, Appendices.

(a). Intrinsic Efficiency Data preceded by explanatory note; graphs giving intrinsic efficiency as a function of source-detector distance for mercury-203 and caesium-137 sources.

(a). Full Energy Peak Intrinsic Efficiency Data for 3.71 cc. planar Ge(Li) Detector.

Explanatory Note on Data Tabulation.

The overall efficiency for detection of gamma-rays of energy E is given by the following ratio:

Number of gamma-rays of energy E recorded in the full energy peak of the spectrum : Total number of gamma-rays of energy E leaving the source in the same time.

Thus, if the total count in the full energy peak, corrected for background, is N, and is accumulated in live time T of the analyser, then the full energy peak counting rate,(n), is (N/T), and the overall efficiency is (n/S). Here S is the source strenth in gammas emitted per second at the time of measurement and is related to the calibration source strength, S_0, by

$$S = S_0 \exp(-0.693t/T_{1/2}),$$

where $T_{1/2}$ is the half-life of the nuclide and t is the time elapsed since the reference time of the source.

The intrinsic efficiency, which is the ratio having the ratio having the same numerator as the overall efficiency, but a denominator which includes only those gammas incident on the detector face, is then given by

$$n.4\pi R^2 / S.A,$$

where A is the area of the face of the encapsulated detector which faces the oncoming radiation, and R is the total distance between the source and the corresponding face of the detector's active volume.

The relative error in the intrinsic efficiency results is given by the equation,

$$(\text{Standard Deviation in Efficiency/Efficiency})^2 =$$

$$(1/N) + 4(\text{S.D. in } R/R)^2 + (\text{S.D. in } S/S)^2$$

where the relative error in S is made up of the given calibrated source error and the error in the gamma-rays per disintegration factor.

If p_o and f are the maximum channel counts and the full width at half maximum, measured in channels, for each peak recorded, then $(1.066 p_o f)$ is the theoretical count rate for a Gaussian peak with parameters p_o and f. In the following tables p_o was also corrected for background.

Data	Source	E(Kev.)	Activity (ucie)	Reference Date	S with percent error	Measurement Date	$T_{1/2}$
A	Hg-203	279.1	20.92	1.i.67.	58.45x $10^4 \pm 1.4\%$	Jan.5-6,1967	46.6±.03d.
B	Cs-137	661.6	10.25	1.i.65.	30.65x $10^4 \pm 2.1\%$	Oct.15-17, 1966	29.82±.11y.
C	Cs-137	661.6	10.59	1.i.67.	32.35x $10^4 \pm 2.1\%$	Dec.19-30, 1966	29.82±.11y.

N.B. The window on the active volume of the detector, measured from the outer face of the cryostat (x), is 0.472 cms. in all cases.

N counts (background corrected).	R cms.	T mins.	P_o counts	f channels	Overall Efficiency ($\times 10^{-4}$)	Intrinsic Efficiency Percent.	Error Percent in Efficiency	$1.066 p_o f$	$(1.066 p_o f - N)/N \times 100\%$	A
52,400	5.55	2	560	85	9.32	5.47±.13	2.3	50,800	-3.0	
82,600	10.63	8	880	88	3.27	7.90±.13	1.7	82,700	+0.1	
50,960	15.71	10	699	72	1.62	8.50±.14	1.6	53,600	+5.2	
126,540	20.79	40	1307	89	0.945	9.24±.14	1.5	124,000	-2.0	
83,100	25.87	40	988	78	0.624	9.39±.14	1.5	82,250	-1.0	
										B
7,554	3.77	1	149	41	4.10	1.38±.05	3.5	6510	-14	
11,283	6.82	4	263	35	1.53	1.69±.05	2.7	9800	-13	
10,496	10.47	8	253	35	0.713	1.86±.05	2.5	9440	-10	
12,480	15.47	20	297	39	0.339	1.93±.05	2.4	12,340	-1.1	
7,273	20.97	20	189	34	0.197	2.05±.05	2.5	6,860	-5.7	

N counts (Background corrected).	R cms.	T mins.	p_o counts	f channels.	Overall Efficiency. ($\times 10^{-6}$)	Intrinsic Efficiency Percent.	Error Percent in Efficiency	$1.066 p_o f$	$(1.066 p_o f - N)/N \times 100\%$	C
91,600	3.09	10	1589	42	472	1.07±.04	3.9	71,200	-22	
159,300	5.63	40	2723	49	205	1.54±.04	2.8	142,000	-11	
104,760	10.63	80	1904	49	67.5	1.81±.04	2.3	99,500	-5.0	
50,540	15.71	80	1141	42	32.5	1.90±.04	2.2	51,100	+1.1	
28,450	20.79	80	689	38	18.3	1.88±.04	2.2	27,900	-1.9	
19,280	25.87	80	440	39	12.4	1.97±.05	2.3	18,350	-4.8	
13,360	30.95	80	343	36	8.60	1.95±.05	2.3	13,200	-1.2	
9,730	36.03	80	242	36	6.26	1.93±.05	2.4	9,300	-4.4	
17,500	41.11	179	396	43	5.04	2.02±.04	2.2	18,200	+4.0	
11,440	46.19	156	294	36	3.77	1.91±.04	2.3	11,280	-1.4	
25,740	41.11	266.5	604	38	4.97	1.99±.04	2.2	24,500	-4.8	
19,815	46.19	263.5	446	40	3.88	1.96±.04	2.2	19,000	-4.1	
28,025	51.27	442.2	637	39	3.26	2.04±.04	2.2	26,500	-5.4	
70,420	56.35	1394	1574	41	2.60	1.96±.04	2.1	68,900	-2.2	

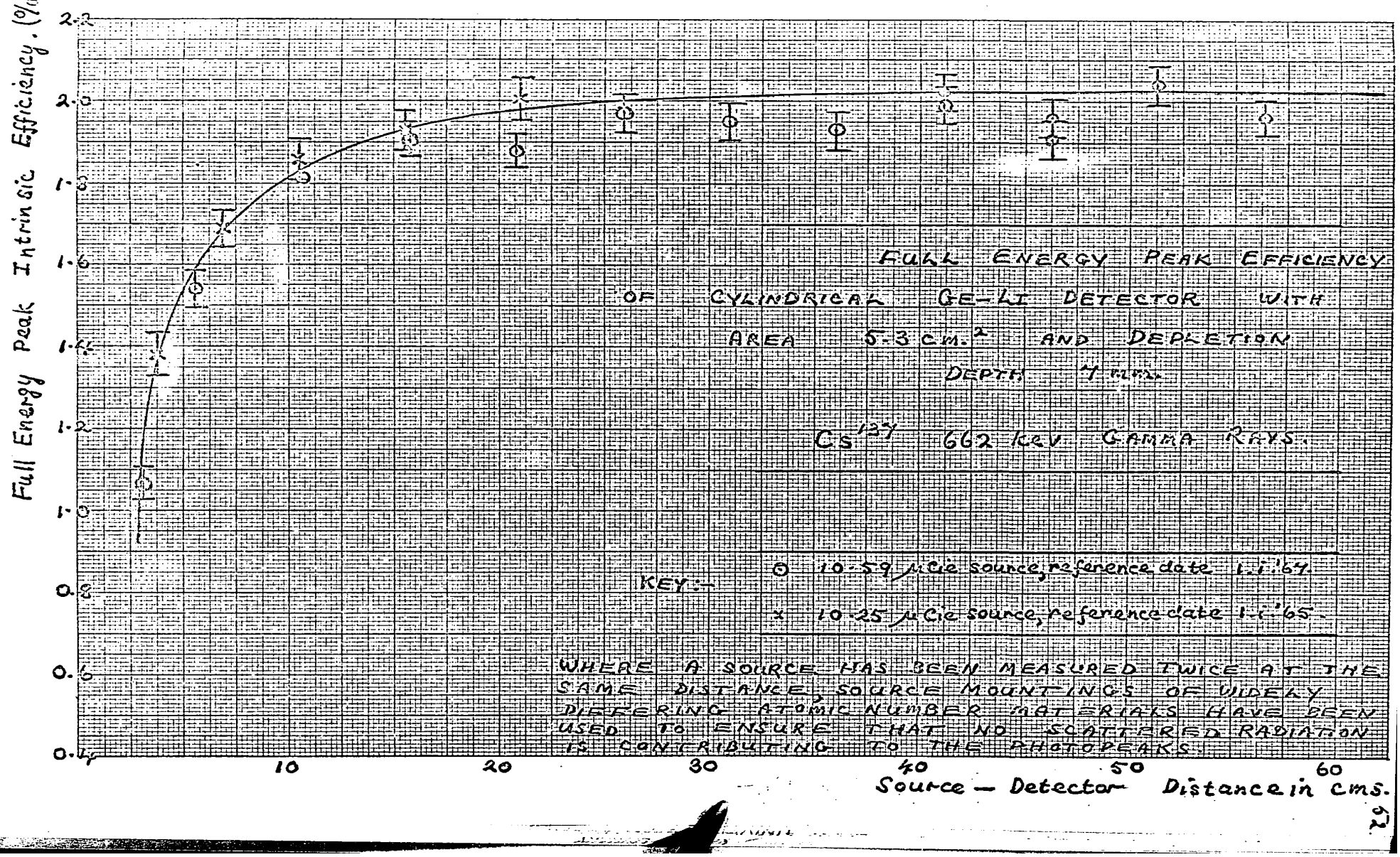
Full Energy Peak Intrinsic Efficiency. (%)
2.2
2.0
1.8
1.6
1.4
1.2
1.0
0.8
0.6
0.4
10
20
30
40
50
60
Source — Detector Distance in cms.
FULL ENERGY PEAK EFFICIENCY
OF CYLINDRICAL GE-LI DETECTOR WITH
AREA 5·3 CM.² AND DEPLETION
DEPTH 7 MM.
Cs¹³⁷ 662 KEV GAMMA RAYS.
KEY:-
⊙ 10·59 μCie source, reference date 1.1.'67.
× 10·25 μCie source, reference date 1.1.'65.
WHERE A SOURCE HAS BEEN MEASURED TWICE AT THE
SAME DISTANCE, SOURCE MOUNTINGS OF WIDELY
DIFFERING ATOMIC NUMBER MATERIALS HAVE BEEN
USED TO ENSURE THAT NO SCATTERED RADIATION
IS CONTRIBUTING TO THE PHOTOPEAKS.

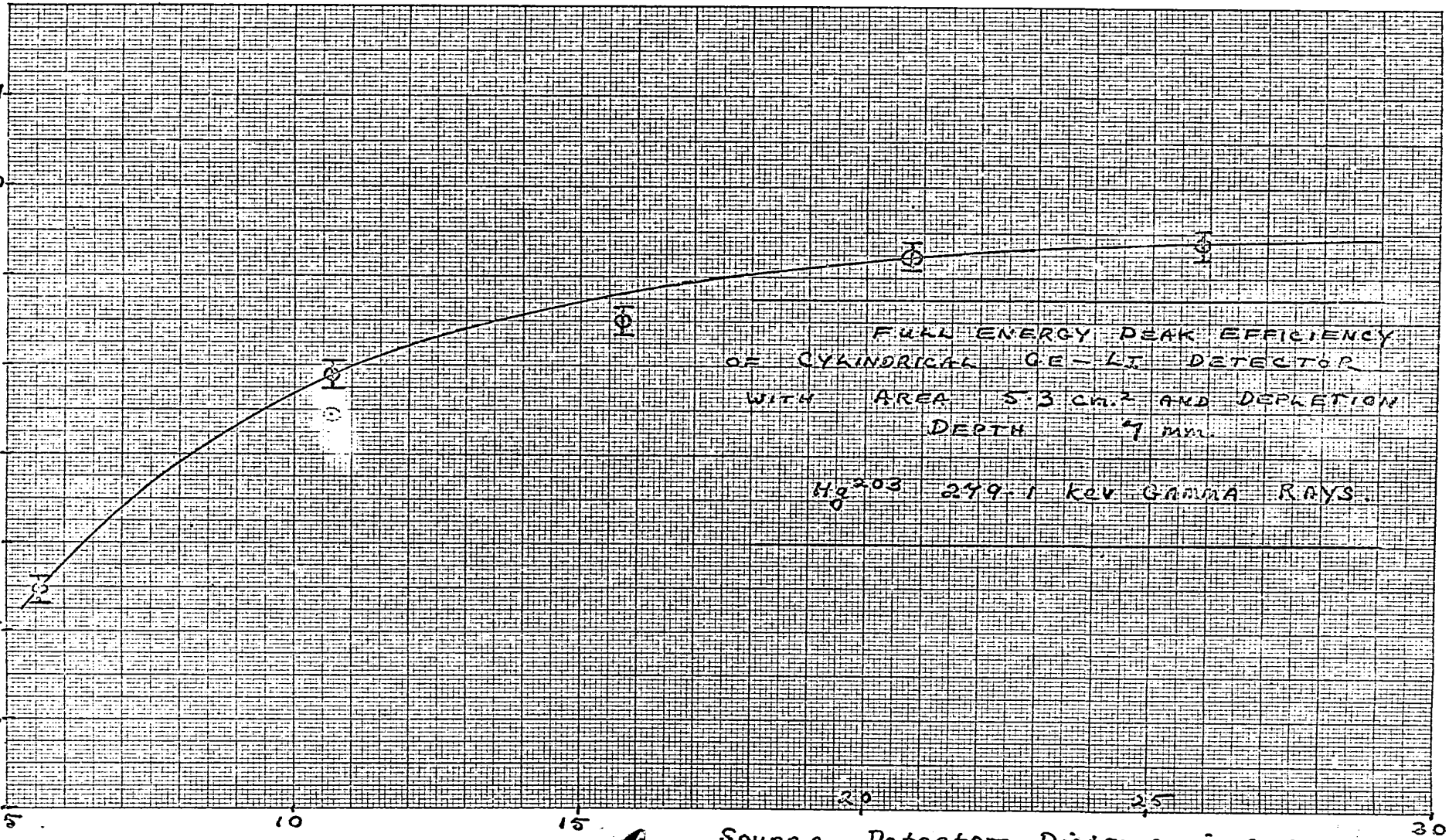

(b) Gamma-Ray Spectrometry Results:

Summary, Tables of Analyser Calibration and Detector Linearity Data, Appendix 1. on analysis of errors in the Linear Interpolation Method ,and Graphical Representation of the Data.

Summary of Gamma-Ray Spectrometry Results.

Date of Measurement	Gamma Source	Previous Measurement	Previous Value(Kev.)	Present Value(Kev.)
July 2nd,1966	Na-22	REF. 5	1274.6± 0.3	1274.1±0.2
July 13th,1966	Na-22	"	1274.6± 0.3	1274.2±0.5
July 5th,1966	Na-22	REF.6,7. (Positron	511.003±.005 annihilation	511.0±0.3 Gammas.)

Summary of Detector Response Data.

Date of Measurement	Gamma Sources Used.	Energy Range Covered. (Kev.)	Slope of Response in Kev. per volt.	Intercept on Energy axis(Kev.)	Maximum Integral Non-Linearity.
July 13th 1966	Mn54,Zn-65,Co-60,Na-22	835 to 1332.	2735.0 ± 3.4	0 ± 1.0	0.1% (Graph 5).
July 2nd 1966	Co-60, Na-22	1173 to 1332	2774.0 ± 3.5		
July 5th 1966	Ir-192 Th(B+C+C' Na-22.	206 to 612.	2725 ± 2.8	- 0.75 ± 0.14	0.5% (Graph 3).

Calibration and Detector Linearity Data (1).

Measurements made on July 2nd., 1966.

Source	E(Kev.)	Peak Channel	Pulser Voltage.	
Calibration Lines.		(± 0.25)		Pulser Voltages are Obtained from Graph 1.
Co-60	1173.23 ±0.04	61.5	0.4283 ± 0.00005	
N.B.(1).	1332.48 ±0.05	346.0	0.4857 ± 0.00005	
Na-22 N.B.(2).	1274.6 ±0.3	241.0	0.4647 ± 0.00005	

N.B. (1). Energies of primary standard gamma-rays were taken from Reference (7).

N.B. (2). The earlier measurement made on this transition is described in Reference (5).

Calibration and Detector Linearity Data (2).

Measurements made on July 5th., 1966.

Source	E(Kev.)	Peak Channel	Pulser Voltage	
Calibration Lines		(± 0.25)	(±0.0001)	
Na-22	511.003±.005	295.5	0.1876	Pulser Voltages are obtained from Graph 2.
Th (B+C+C")	238.624±.009	71.5	0.0880	
	583.139±.023	357.25	0.2143	
Ir-192	205.740	43.5	0.0750	
	295.938±.009	117.5	0.1087	
	308.429±.010	127.75	0.1134	
	316.486±.010	135.5	0.1170	
	468.053±.014	259.0	0.1717	
	588.557±.017	361.75	0.2162	
	604.385±.017	375.5	0.2222	
	612.435±.017	381.75	0.2247	

Energies are quoted from Reference (7). Maximum detector non-linearity occurring (GRaph 3.) is about 0.5%.

Calibration and Detector Linearity Data (3).

Measurements made on July 13th., 1966.

Source	E(KEV.)	Peak Channel	Pulser Voltage	
Calibration Lines		± 0.25	±0.00014	Pulser Voltages are obtained from Graph 4.
Mn-54	835.0±0.3	53.0	0.3050	
Zn-65	1115.6±0.4	235.0	0.4076	
Co-60	1173.23±0.04	272.25	0.4285	
Na-22	1274.6±0.3	338.0	0.4656	
Co-60	1332.48±.05	375.5	0.4870	

Energies of Co-60 primary standard gamma-rays were taken from reference (7), the remainder from reference (5). Maximum detector non-linearity occurring (Graph 5) is about 0.1%.

Appendix 1.

The calculation of an unknown gamma-ray energy, and its standard deviation resulting from the errors in the known calibration lines and the reading errors of the peak channels.

If A,B, and E are the energies of the calibration lines and the line whose energy is being measured , respectively , and a, b, & e are the corresponding peak channel numbers, then linear interpolation gives the relation

$$(E-B)/(A-B) = (e-b)/(a-b),$$

$$\text{or,} \qquad E = (A-B)(e-b)/(a-b) + B$$

The energy results given in Chapter 3. have been calculated from this formula and their standard deviations (s) from the following function:

$$\left\{ E_A^2 s_A^2 + E_B^2 s_B^2 + E_a^2 s_a^2 + E_b^2 s_b^2 + E_e^2 s_e^2 \right\}^{1/2},$$

where E_A is the partial derivative of E w.r.t. A and S_A is the standard deviation in A, etc.

It can be shown that

$$E_A = (e - b)/(a - b),$$

$$E_B = (a - e)/(a - b),$$

$$E_a = (B - A)(e - b)/(a - b)^2 = -E_A \cdot E_e ,$$

$$E_b = (A - B)(e - a)/(a-b)^2 = -E_B \cdot E_e ,$$

$$E_e = (A - B)/(a - b).$$

There follows a tabulation of the various partial derivatives and constants giving the standard deviations in the results for the various gamma-spectrometry data.

Date	A	B	a	b	e
July 2nd.	1332.48	1173.23	0.4857	0.4283	0.4647
July 5th.	612.435	238.624	0.2247	0.0880	0.1876
July 13th. 1966	1332.48	1173.23	0.4870	0.4285	0.4656

Date	s A	s B	s a	s b	s e
July 2nd.	0.05	0.04	.00005	.00005	.00005
July 5th.	0.017	0.009	0.0001	0.0001	0.0001
July 13th. 1966.	0.05	0.04	0.00014	0.00014	0.00014

Date	E_A	E_B	E_a	E_b	E_e	s
July 2nd.	0.634	0.3655	-1758	-1014	2772	0.175
July 5th.	0.728	0.2715	-1985	-742	2733	0.34
July13th. 1966.	0.634	0.366	-1725	-998	2725	0.475

Appendix 1. (continued).

The above analysis is a slight simplification of the physical facts in that gamma- energies are measured in terms of their linearly related equivalent pulse heights in volts, rather than channel numbers to which they are not strictly linearly related due to the non-linear processes involved, mentioned in chapter 3 (b). However, since these pulse heights are determined from a channel number versus voltage graphical relation, and since the error in an isolated voltage reading is restricted to that in the Keithley differential voltmeter, i.e. one part in 5000, the relative errors in the voltage differences derived from the graph are very close to the relative errors in readings of the intervals, in channel numbers, between the corresponding gamma peaks on the analyser display. The above error analysis is thus perfectly valid.

GRAPH 1.

PULSER CALIBRATION.
ENERGY RANGE: 1173 — 1332 KEV.
DATE OF MEASUREMENT: JULY 2ND, 1966
EXPERIMENTAL ERRORS :—
CA. 1/5 MM.
{± 1/4 channel and ± 10⁻⁴ volts}
Co 60
Na 22
Co 60
CHANNEL NUMBER OF PEAK.
400
360
320
280
240
200
160
120
80
40
.496
.480
.464
.448
.432
.416
.400
PULSER VOLTAGE — VOLTMETER READING.

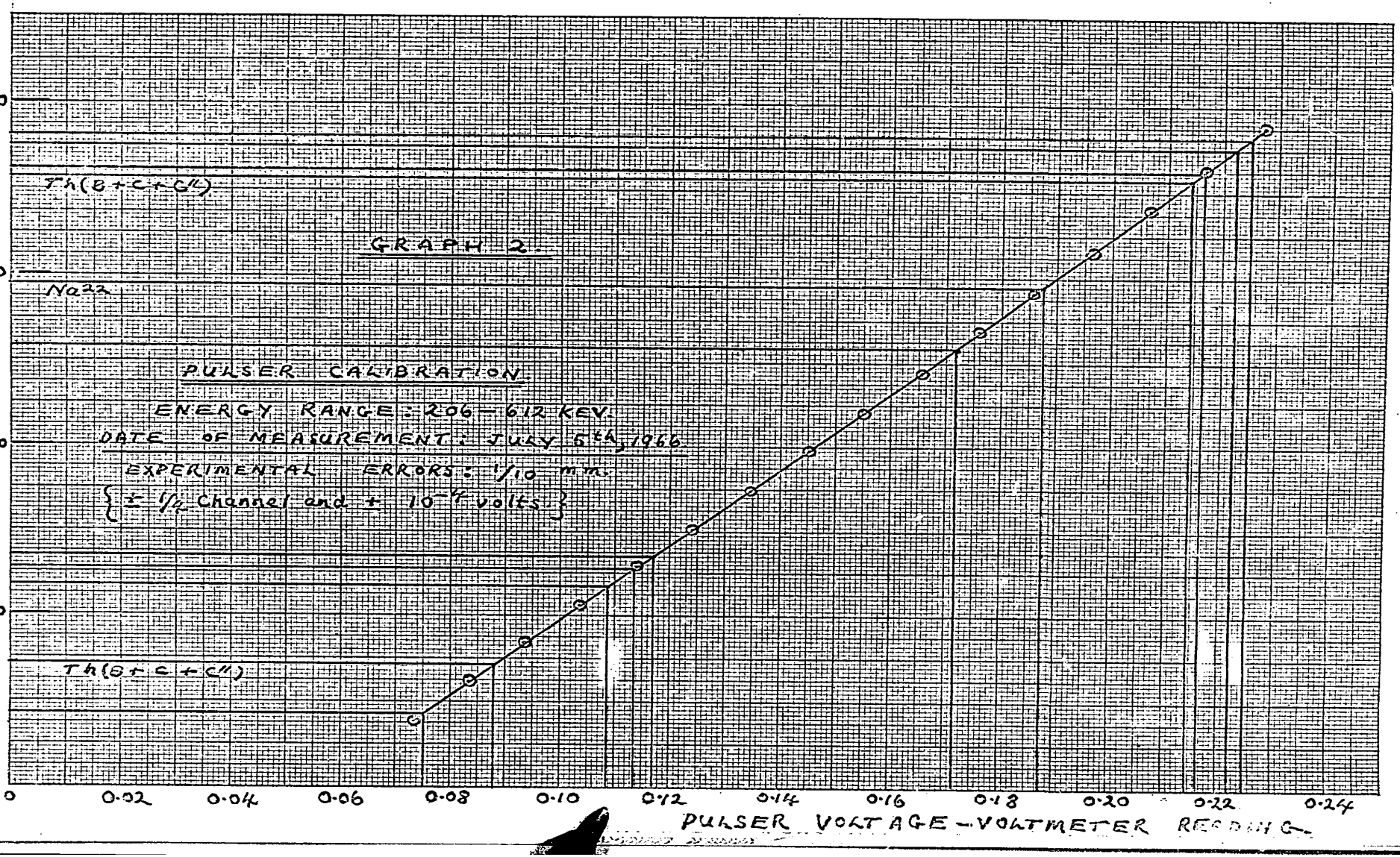

GRAPH 3.

DETECTOR LINEARITY.

SOURCES USED: I_r^{192}, Th(B+C+C') and Na^{22} (annihilation radiation)

DATE OF MEASUREMENT: JULY 5th 1966

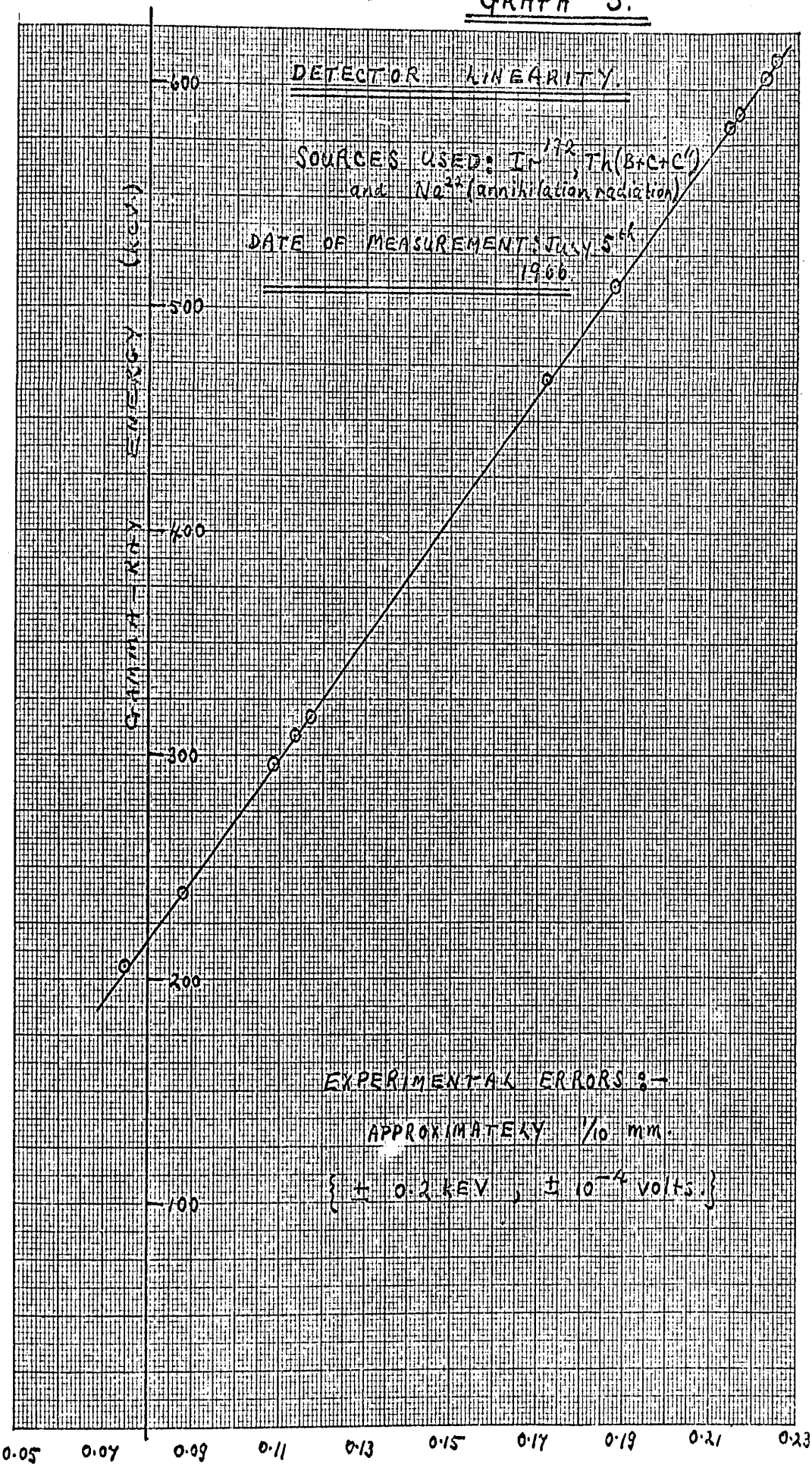

EXPERIMENTAL ERRORS :–

APPROXIMATELY 1/10 mm.

{ ± 0.2 KEV , ± 10^{-4} volts }

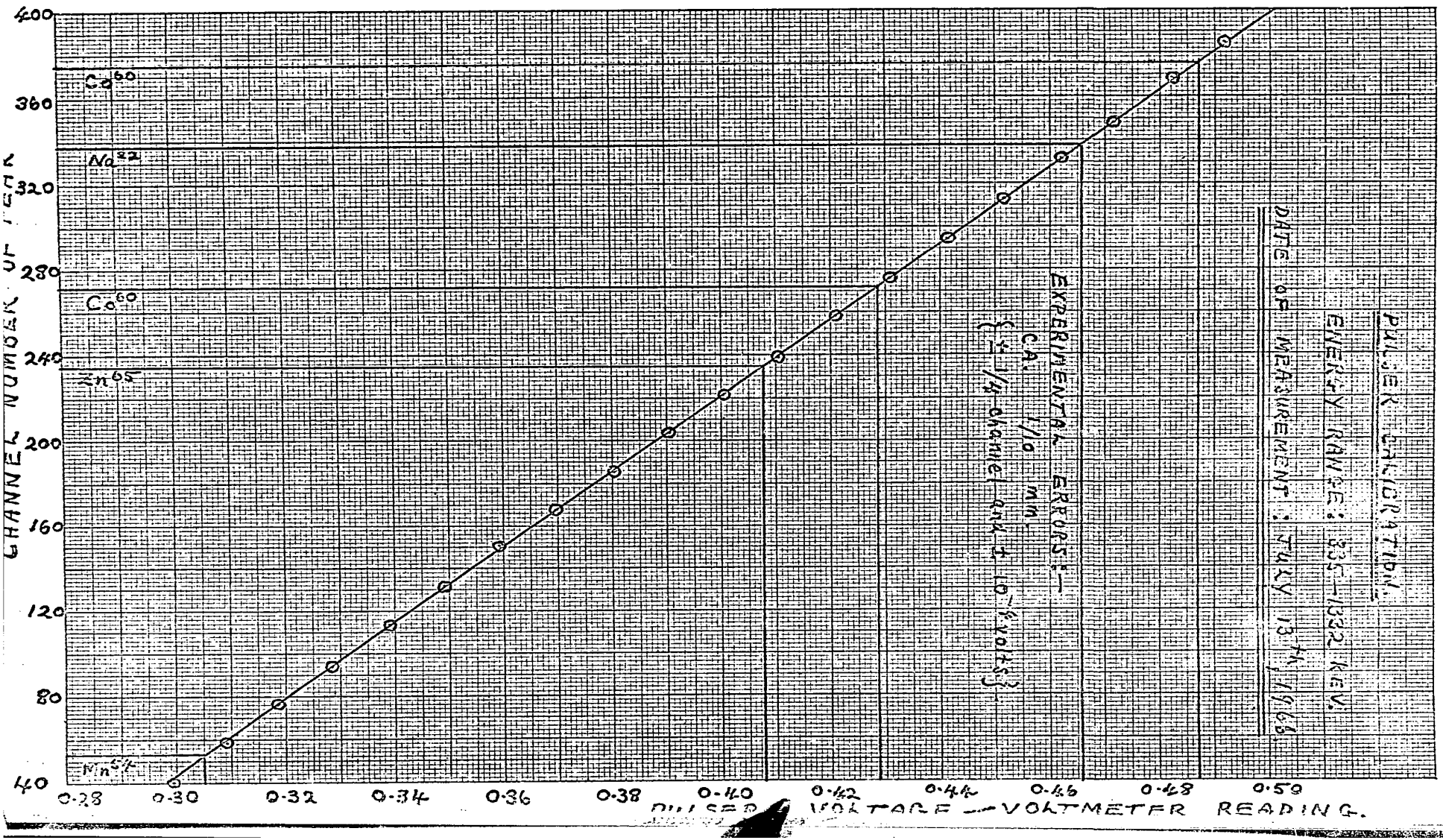

GRAPH 4.

GRAPH 5.

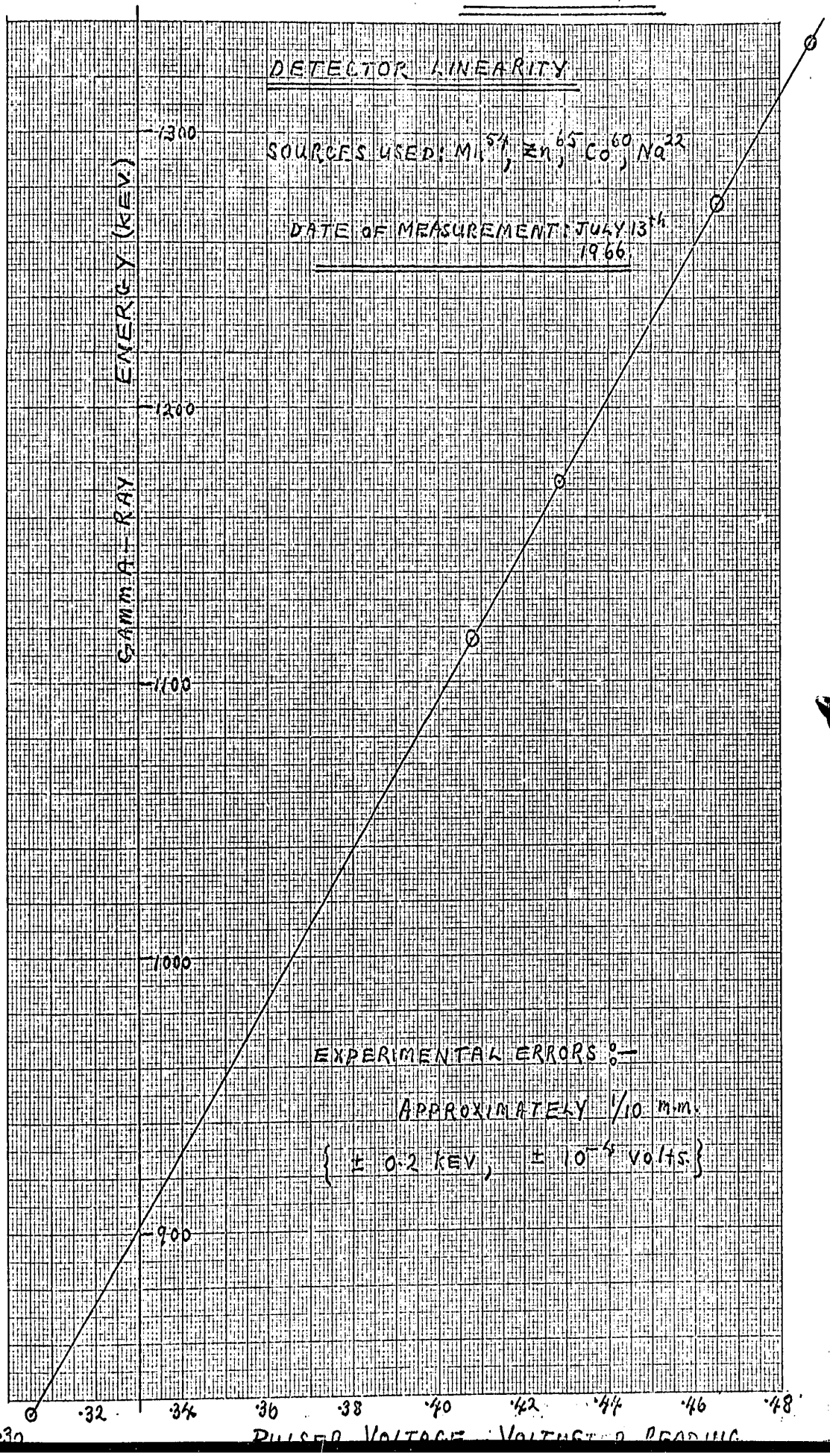

(c). Energy Resolution Data and plot of relation giving Fano factor of Germanium.

(c). Summarised Data on resolution obtained in Gamma-Ray energy measurements together with Pulser Pulse widths.

Source	Energy (Mev.)	F.W.H.M. (Kev.) (total).	F.W.H.M. (Kev.) (Pulser).	F.W.H.M. (Kev.) (Detector).
Co-60	1.33	3.7	2.43	7.8
		3.7	2.5	7.45
		3.7	2.4	7.94
		4.07	2.37	10.98
		3.60	2.32	7.58
Co-60	1.17	3.96	2.43	9.79
		3.8	2.5	8.19
		3.8	2.4	8.68
		3.74	2.37	8.38
		3.65	2.14	8.75
Co-57	.122	2.43	2.07	1.61
	.136	1.86	2.07	
Na-22	1.275	4.04	3.20	6.10
		4.5	2.32	14.87
Tl-208	2.614	5.85	3.1	24.59
	2.103	5.68	3.1	22.64
Y-88	1.836	3.95	2.23	10.6

Source	Energy (Mev.)	F.W.H.M. (Total).	F.W.H.M. (Pulser).	$(f.w.h.m.)^2$ (detector).
Mn-54	.835	3.54	2.32	7.15
Zn-65	1.116	4.2	2.32	12.2

By plotting the mean values of squared detector half-widths against gamma-ray energies in Mev., F is obtained from the slope, which is 15.75F. The magnitude of the uncertainty in the F result has been found by selecting the best and worst straight lines through the points on the graph.

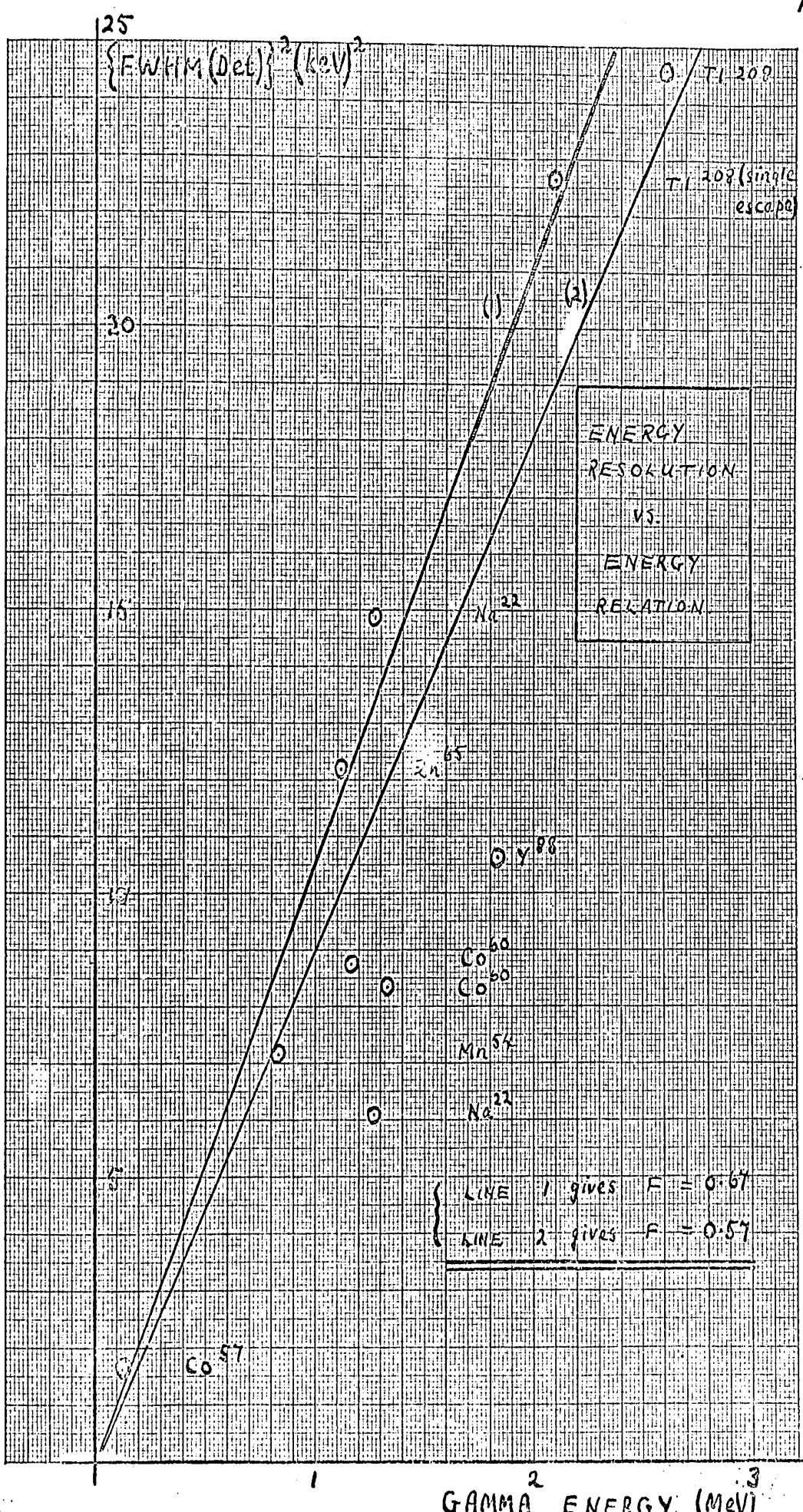

(d). Appendix 2. Heat Transfer between concentric cylinders at Reduced Pressure.

The pressure in the cryostat under operating conditions is between 10^{-3} and 10^{-4} torr. At this pressure the heat transfer between the outer brass case of the cryostat and the inner cylindrical copper cold finger takes place by free molecular conduction and radiation. The former process involves direct transfer of energy from one solid surface to another by transfer of kinetic energy picked up by gas molecules on bombardment of the hotter solid surface and subsequently delivered to the cooler surface after the molecules have traversed the space between the surfaces unhindered by the intermolecular collisions which occur at higher pressures. The latter process is the familiar one of radiative heat transfer which follows Stefan's Law.

The following theory demonstrates that at the pressure used in the cryostat in this work, heat conduction is a relatively unimportant effect in comparison with radiation of heat, which means that further improvement in vacuum is unnecessary and not worthwhile.

Dushman(REF. C, pp. 52-55) gives the following formula for heat transfer by conduction at reduced pressures between concentric cylinders of radii (a) and (r) ($r > a$), per unit area of the inner cylindrical surface as

$$E_0 = \alpha_r \Lambda P(273.2/T_a)^{1/2}.(T_r - T_a)$$

where Λ is the free molecule heat conductivity at 0°C, given by

$$\frac{1.468 \times 10^{-5}}{(M)^{1/2}} \cdot \left(\frac{\gamma + 1}{\gamma - 1}\right) \text{ watts.cm}^{-2}\text{.deg.}^{-1}\text{micron}^{-1},$$

and P is the gas pressure in microns of mercury between the cylinders, T_r and T_a are the temperatures of the surfaces of radii r(4cms.) and a(1cm.), and α_r is a function of the accommodation coefficient, α, of the surfaces , which takes account of the fact that the mean energy

of gas molecules after contact with those of the surface material does not quite reach a level corresponding to the temperature of that surface. Thus the true temperature, T, of molecules re-emitted from a surface at temperature T_s after incidence at temperature T_i is given by

$$\alpha = (T-T_i)/(T_s-T_i).$$

α is approximately 0.9 for air on surfaces of the kind used in the cryostat and α_r is given by

$$\alpha / \{1-(1-\alpha)(a/r)\} ,$$

which is 0.924 for the cryostat geometry. Using the above data the value E_o of heat gain per unit area of the cold finger by conduction through air in the upper part of the cryostat is approximately 0.45×10^{-3} watts per $cm.^2$ at 10^{-4} torr. and 4.5×10^{-3} watts per $cm.^2$ at 10^{-3} torr.

The corresponding figure for radiative heat transfer is given by

$$E_{rad.} \doteq \varepsilon \sigma (T_r^4 - T_a^4)$$

where ε is the emissivity of the inner surface (taken as 0.3 for copper (ref. D)), σ is Stefan's constant, 5.7×10^{-12} ergs/$(°K.)^4.cm.^2$sec. and T_r and T_a are measured in degrees Kelvin.

Thus, $E_{rad.} = 11 \times 10^{-3}$ watts/$cm.^2$ when T_r is 283°K and T_a is 100°K.

The above formula is strictly only true in the case when $a \ll r$, when the outer surface behaves as a black body, reflecting no energy back to the inner cylinder. In the present case (r/a) is about 4 and the above formula should be sufficiently accurate for this order of magnitude calculation. Also it is assumed here that no significant heat transfer takes place in the lower part of the cryostat where the outer cylinder is in contact with liquid nitrogen and is thus close in temperature to the cold finger.

The foregoing shows that at 10^{-3} torr the two processes give rise to similar amounts of heat transfer whereas at 10^{-4} torr radiative transfer

accounts for approximately 96% of the total heat transfer.

(e). Representative Examples of Spectral Peaks used in Efficiency Measurements.

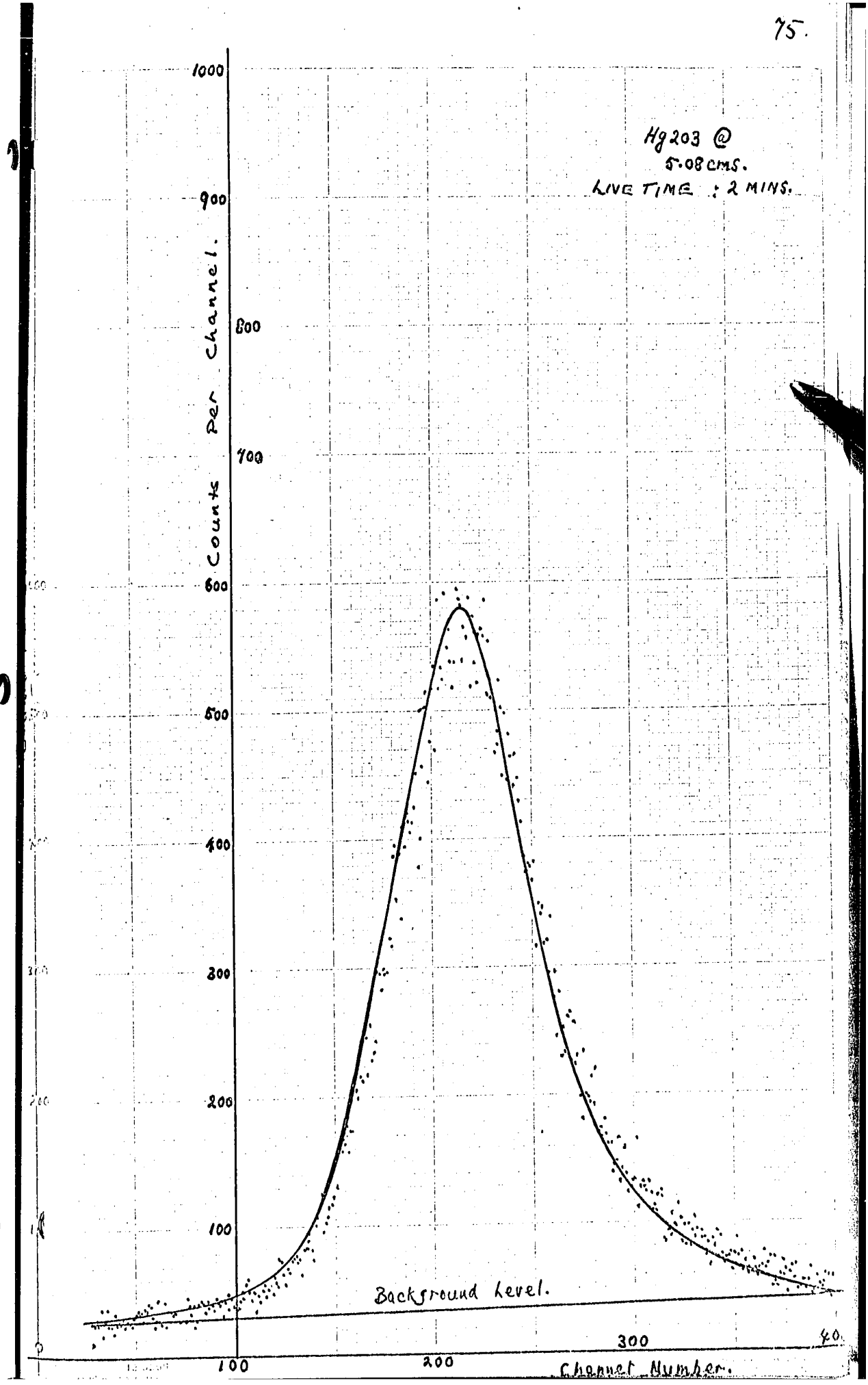
Hg 203 @
5·08 cms.
LIVE TIME : 2 MINS.
Counts Per Channel.
1000
900
800
700
600
500
400
300
200
100
0
Background Level.
100
200
300
Channel Number.

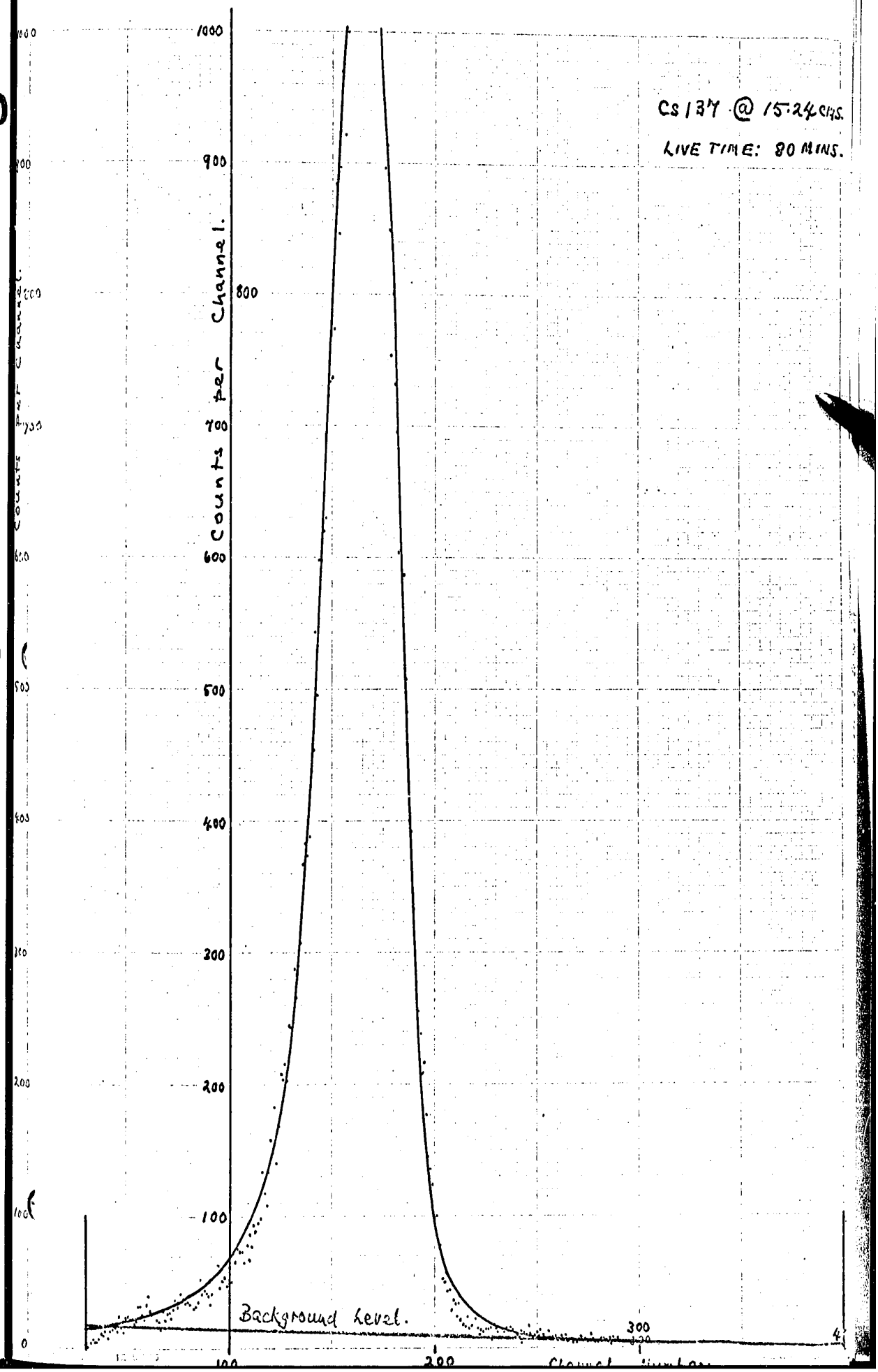
Cs 137 @ 15.24 cms.
LIVE TIME: 80 MINS.
Counts per Channel.
1000
900
800
700
600
500
400
300
200
100
0
Background Level.
100
200
300
Channel number.

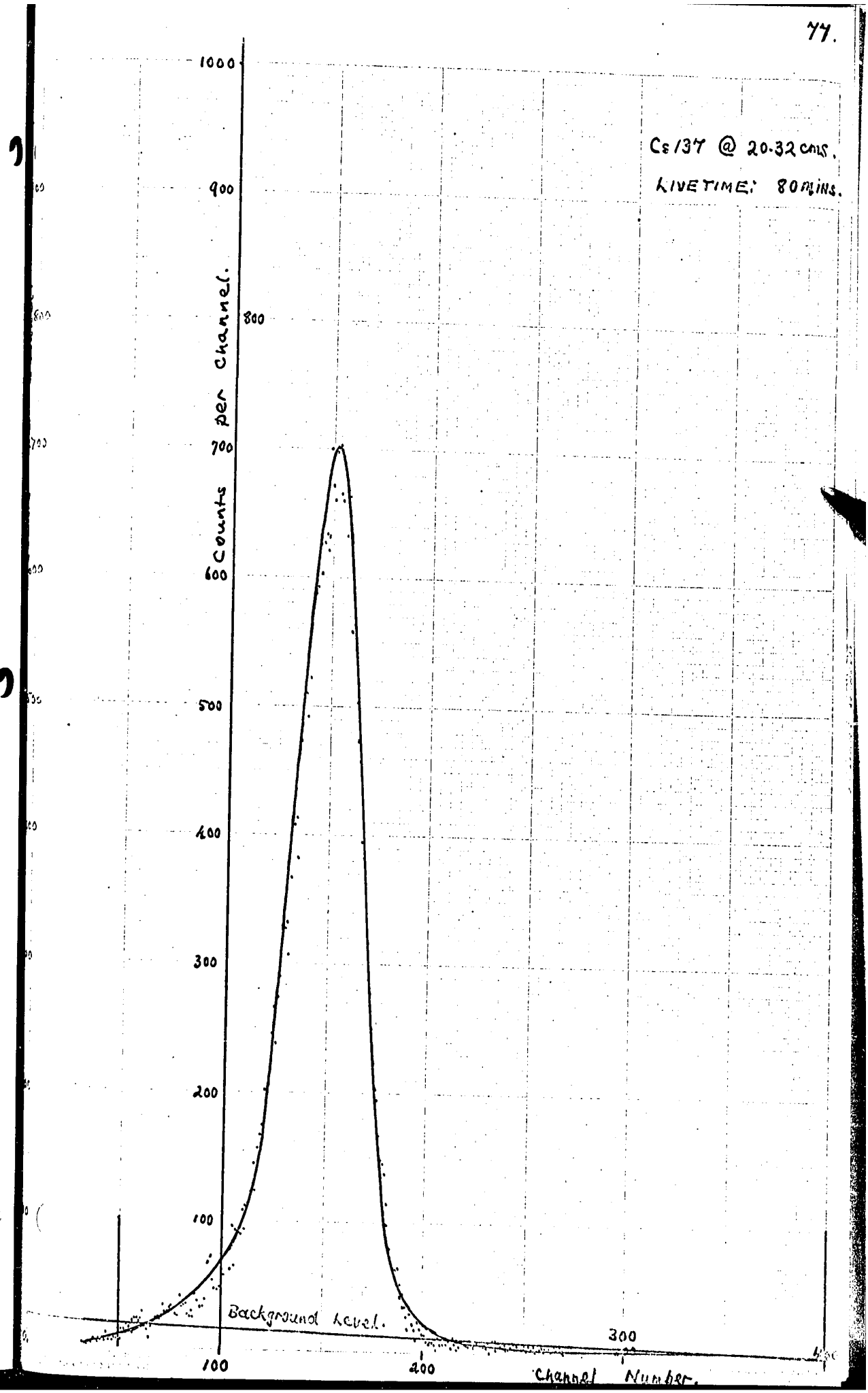
Cs/37 @ 20.32 cms.
LIVETIME: 80 MINS.
Counts per Channel.
1000
900
800
700
600
500
400
300
200
100
Background level.
100
200
300
Channel Number.

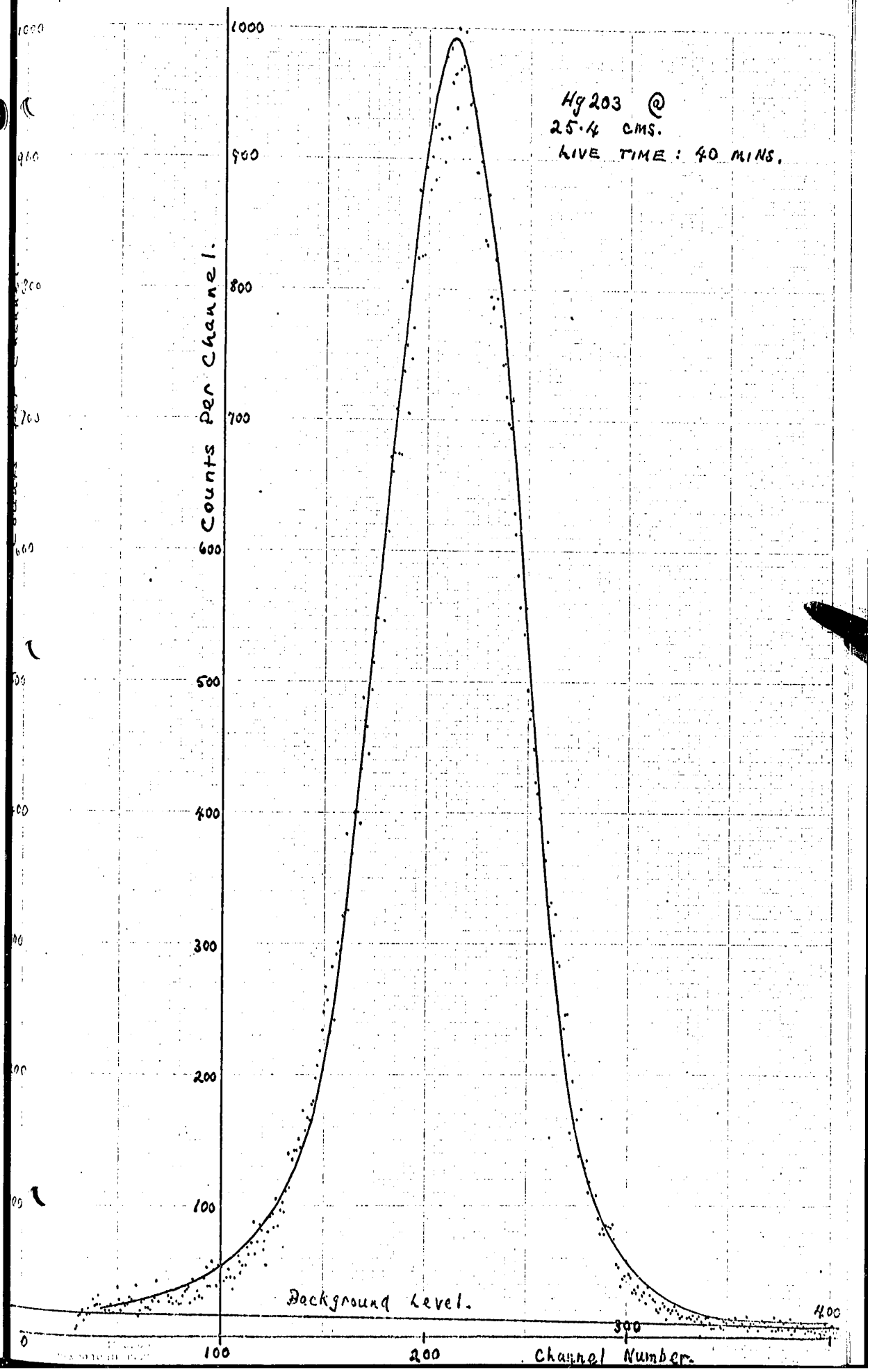
Hg 203 @
25·4 cms.
LIVE TIME : 40 MINS.
Counts per Channel.
1000
900
800
700
600
500
400
300
200
100
Background Level.
0
100
200
300
400
Channel Number.

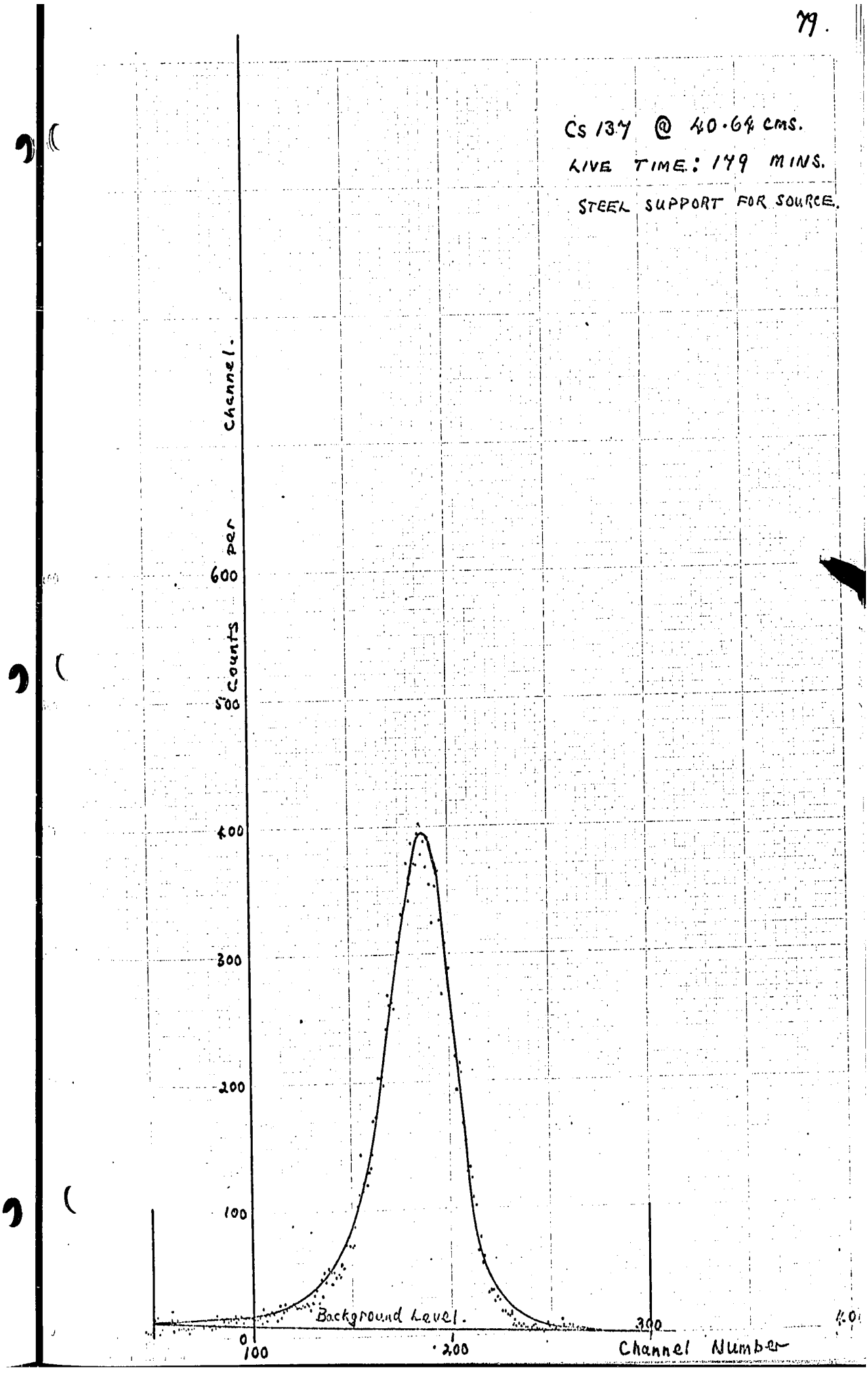
Cs 137 @ 40·64 cms.
LIVE TIME: 149 MINS.
STEEL SUPPORT FOR SOURCE.
Channel.
600
500
400
300
200
100
Counts per
Background Level.
0
100
200
300
Channel Number

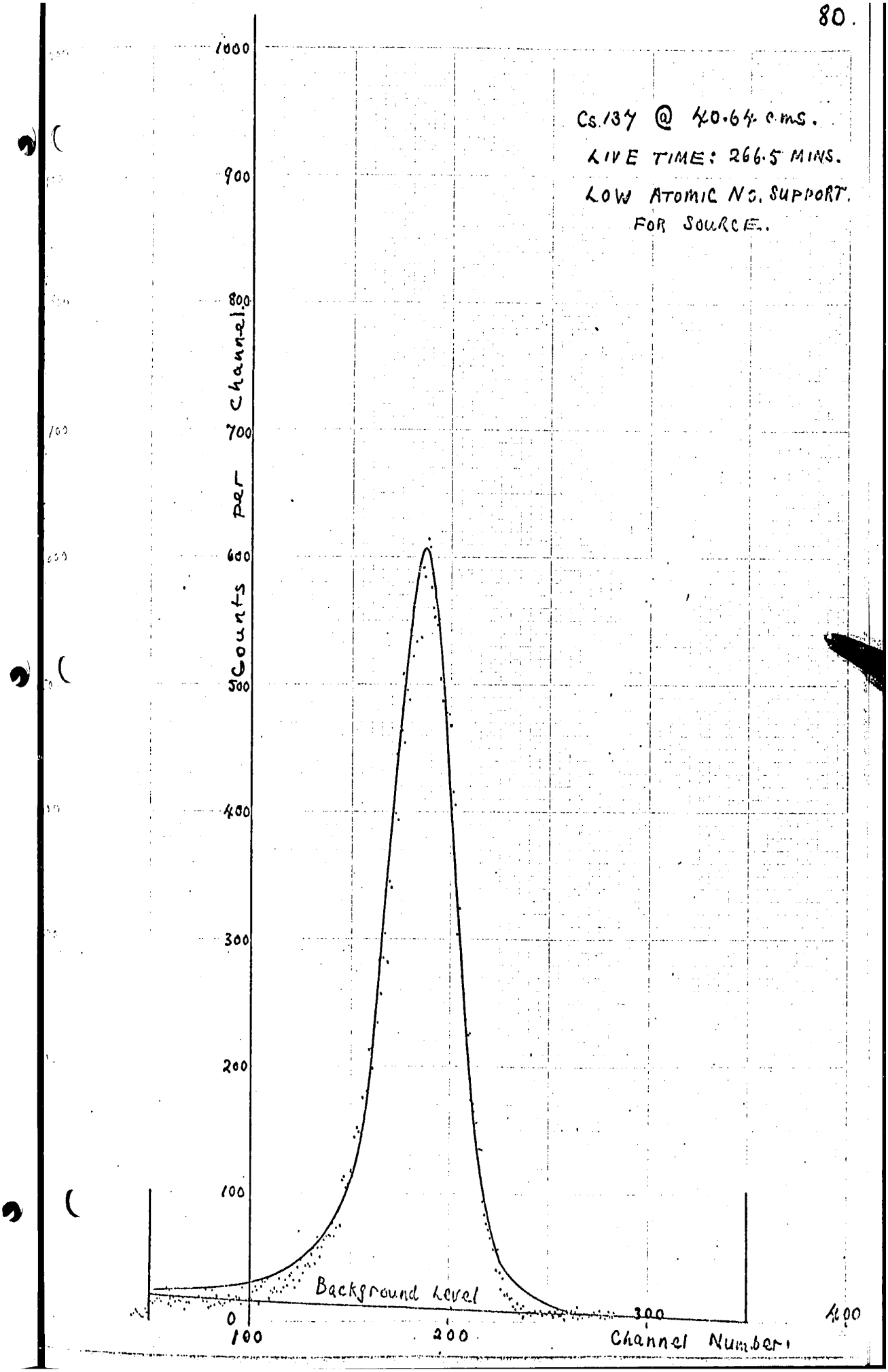
Cs.137 @ 40.64 cms.
LIVE TIME: 266.5 MINS.
LOW ATOMIC No. SUPPORT.
FOR SOURCE.
Counts per Channel
1000
900
800
700
600
500
400
300
200
100
0
Background Level
100
200
300
400
Channel Number

Section 9. List of References.

General References.

(A). Semiconductor counters for Nuclear Radiations.

Dearnaley and Northrop. (Spon).

(B). Radioactive Isotopes.

Whitehouse and Putnam. (O.U.P.)

(C). Foundations of Vacuum Technique.

Saul Dushman. (Wiley.)

(D). Elements of Physics.

A.W.Smith and J.N.Cooper. 7th Edition.

(McGraw-Hill).

Specific References.

(1). D.V.Freck and J. Wakefield,

Nature, 193, (1962),669.

(2). P.Webb and R.L.Williams,

Nuclear Instruments and Methods, 22,(1963),361-2.

(3). G.T.Ewan and A.J.Tavendale,

Canadian Journal of Physics, 42,(1964),2286-2329.

(4). H.L.Malm, A.J.Tavendale, and I.L.Fowler,

Canadian Journal of Physics, 43,(1965), 1173-1181.

(5). R.L.Robinson, et alia,

Nuclear Physics, 74,(1964), 281-288.

(6). E.R.Cohen, J.W.M.Dumond,et alia,

Reviews of Modern Physics, 27,(1955),363.

(7). G.Murray, R.L.Graham, and J.S.Geiger,

Nuclear Physics,63,(1965), 353-382.

(8). I.L.Fowler, Canadian Nuclear Technology,

Winter 1965,40-44.

(9). C.Chasman and R.A.Ristinen,

Brookhaven National Laboratory Report B.N.L. 8692,(1964).

(10). T.M.Dauphinee and H.Preston-Thomas,

Review of Scientific Instruments,25,No.9,(1954),884-886.

(11). F.S.Goulding,

Nuclear Instruments and Methods,43,1966.

Section 10. Vita.

Name: Jeffery Alan Chaplin.

Born: Ilford, Essex, England, 1940.

Education:

Primary: South Park Primary & Junior School, Seven Kings, Essex, England, 1945 - 1950.

Secondary: Brentwood School, Brentwood, Essex, England, 1950 - 1958.

University: (1). Clare College, Cambridge, 1959 - 1962. B.A.(Hons.), 1962. Parts 1 & 2, Natural Sciences Tripos. (Part 2, Physics.)

(2). Reactor Physics Department, The University, Birmingham 15, England, 1963 - 1964. M.Sc. degree, 1964, in Reactor Physics and Technology by examination, research & report.

Scholarships & Awards:

1959 - 1962: State Scholarship and Major Open Entrance Scholarship, to Clare College, Cambridge.

1963 - 1964: D.S.I.R. Advanced Course Studentship, to the University of Birmingham.

1965 - 1966: Ontario Graduate Fellowship, University of Ottawa.

1964 - 1965 and 1966 - 1967: University of Ottawa Graduate Assistantships.

Appointments: 1962 - 1963: Research Assistant in Oceanography, Department of Geodesy and Geophysics, Cambridge University, England.

October 1967 - present: Scientific Officer, Department of Energy, Mines and Resources,

Appointments,(cont'd):

Geological Survey Branch, Ottawa, Canada.

Theses:

(1). In partial fulfillment of the M.Sc. degree requirements of the University of Birmingham, a thesis entitled "The Velocity of Sound in Two-Phase Media" 1964.

(2). The present thesis.